The Application of Ultrasonic NDT Techniques in Tribology

Review Paper

R.S. Dwyer-Joyce
Department of Mechanical Engineering,
The University of Sheffield,
Mappin Street, Sheffield, S1 3JD, UK.
r.dwyerjoyce@sheffield.ac.uk

Keywords

Ultrasound, tribology, real area of contact, contact stress measurement, lubricant film measurement, review

Abstract

The use of ultrasonic reflection is emerging as a technique for studying tribological contacts. Ultrasonic waves can be transmitted non-destructively through machine components and their behaviour at an interface can describe characteristics of that contact. This paper is a review of the current state of understanding of the mechanisms of ultrasonic reflection at interfaces; and how this has been used to investigate the processes of dry rough surface contact and lubricated contact. The review extends to cover how ultrasound has been used to study the tribological function of certain engineering machine elements.

1. Introduction

The nature of the interface between two solid materials is at the very centre of tribology. If the interface is unlubricated, then the way the asperities contact and the resulting true area of contact is important information. Without this it is not possible to predict or effectively model, contact stress, friction, contact fatigue, or wear. On the other hand, if the tribological interface is lubricated, then the thickness of that lubricating film and its physical properties are important. The successful protection of the contacting surfaces relies on the integrity and performance of the oil film.

Despite the fundamental nature of these requirements, experimental methods for their measurement have proved difficult to achieve. The problem is one of scale; asperity contacts are small and lubricant films are thin compared with the dimensions of the components they separate. Since conventional geometrical metrology tools are not suitable, the measurements require the transmission of some form of independent signal across the interface.

Electricity, heat, and light have all been used for these measurements and significant progress has been made. However, these methods require substantial modification to the component; either with the need for transparency, electrical isolation, or the use of surface mounted sensors. This review is concerned with the use of ultrasound as the measurement medium. The reflection or transmission of a high frequency displacement wave (an ultrasonic pulse) at an interface does not suffer from these disadvantages. The approach can be used flexibly on many (but not all) real engineering materials and components.

When an ultrasonic wave strikes an interface it is either entirely or partially reflected. This

phenomenon is widely used in non-destructive testing; where ultrasound is commonly used for inspection of cracks, internal flaws, and defects. There is a large body of work on the transmission, reflection, attenuation, and scattering of such acoustic waves in structures and liquids (see for example Kräutkramer & Kräutkramer 1975, Povey 1997).

The kind of interfaces that concern tribologists, dry and lubricated machine element contacts, can be also measured in this way. A dry contact between two machine elements presents an interface consisting of individual asperity contacts and air gaps. A lubricated contact presents an interface consisting of a thin film trapped between two solid materials.

The review is divided into three parts; firstly, the development of the theoretical tools that have allowed the interpretation of reflected (or transmitted) ultrasound at a dry or lubricated tribological interface; secondly, how these tools have been used to understand more about dry contacts; and thirdly, some examples of where these techniques have found applications in machine element tribology.

2. The Response of a Tribological Interface to an Ultrasonic Wave

Ultrasound is a displacement wave at frequencies higher than those of human hearing. The waves are usually generated by the excitation of a piezo-electric material by a voltage pulse. The voltage causes the transducer to deflect. If the transducer is bonded or coupled to a solid structure then a mechanical displacement is propagated through the body.

The two most common wave forms are longitudinal (where the vibration of the material is parallel to the direction of wave travel) and shear or transverse (where the vibration of the material is perpendicular to the direction of wave travel).

2.1 The Reflection of Ultrasonic Waves at an Interface

When an ultrasonic wave strikes a complete (i.e. perfectly bonded) interface between two materials it is partially reflected (see figure 1a). The proportion of the wave amplitude that is reflected is known as the reflection coefficient, *R*.

The magnitude of the reflection coefficient depends on the relative mismatch between the acoustic impedances of the two materials (the acoustic impedance, *z* is the product of the density, ρ and the speed of sound in the material, *c*) according to:

$$R = \frac{z_1 - z_2}{z_1 + z_2} \tag{1}$$

where suffices 1 and 2 refer to the materials either side of the interface. If the interface is not perfectly bonded or there is a thin layer (thin compared with the wavelength of the ultrasound), then the proportion of the wave reflected is increased (see figures 1b & c).

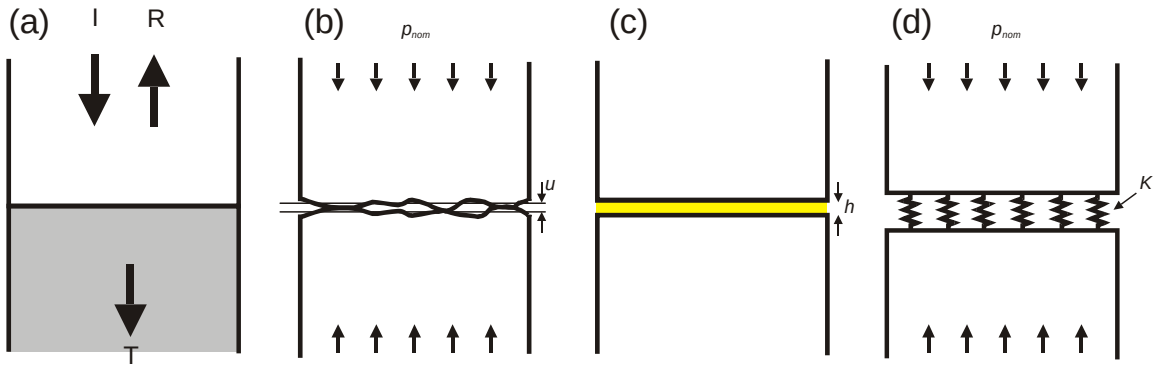

Figure 1 Reflection from interfaces (a) between perfectly bonded materials, (b) between partially bonded materials – rough surface contacts, (c) with a thin layer – lubricated contacts, and (d) the spring model assumption.

A model for the reflection from such an interface was described by Kendal and Tabor (1971) working on rough surface contact. They used a quasi-static approach to demonstrate that the reflection is a function of the stiffness of the interface, *K* (figure 1d). Tattersall (1973), working on thin adhesive layers, came up with the same result. The reflection coefficient is then given by:

$$R = \frac{z_1 - z_2 + i\omega(z_1 z_2 / K)}{z_1 + z_2 + i\omega(z_1 z_2 / K)} \tag{2}$$

The modulus of the reflection coefficient is then:

$$|R| = \sqrt{\frac{(\omega z_1 z_2)^2 + K^2 (z_1 - z_2)^2}{(\omega z_1 z_2)^2 + K^2 (z_1 + z_2)^2}} \tag{3}$$

If the materials either side of the interface are identical, then this reduces to a simple relationship between reflection coefficient and stiffness:

$$|R| = \frac{1}{\sqrt{1 + (2K/\omega z)^2}} \tag{4}$$

Figure 2 shows a plot of the reflection coefficient, predicted by equation 4, against frequency as the stiffness of the interface is varied.

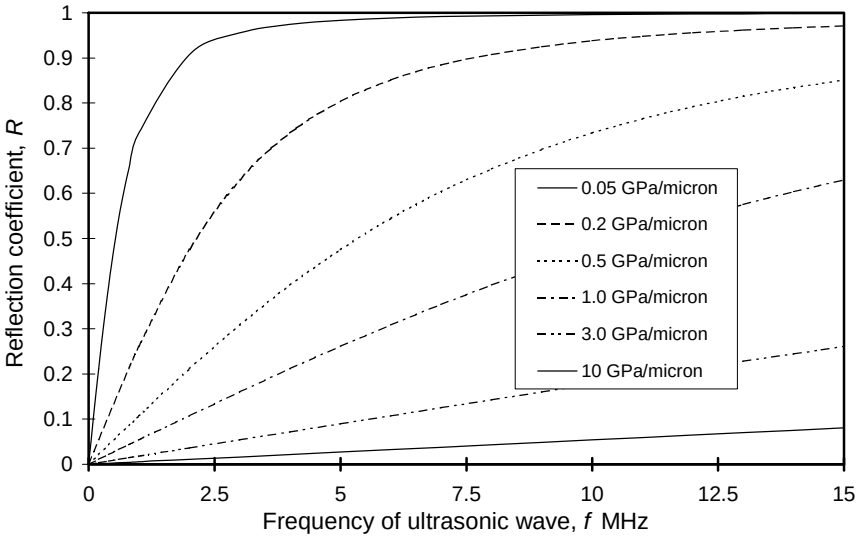

Figure 2 . The response of an interface to an ultrasonic wave (determined for a steel/steel contact) according to the quasi-static spring model equation (4). As the interface becomes stiffer less of the wave is reflected.

2.2. The Stiffness of an Interface

A critical parameter in the ultrasonic response of a contact is the interface stiffness. This is defined as the nominal pressure, p_{nom} require to cause unit approach of the surface mean lines, u:

$$K = -\frac{\mathrm{d}\, p_{nom}}{\mathrm{d}\, u} \tag{5}$$

For a rough surface contact, this is a non-linear parameter. As the load on a contact increases more asperities come into contact and the stiffness increases. The stiffness thus varies from zero (when there is vanishingly little contact) to infinity (when there is complete contact across the interface). It should be noted that this is a distributed stiffness (i.e. a stiffness per unit area of the interface). Convenient units are GPa/μm, since in tribology, pressures in giga-Pascals cause displacements of the order of microns.

If the interface consists of a layer of liquid (i.e. a lubricant) then the stiffness is determined from the layer bulk modulus, B and the thickness of the layer, h:

$$K = \frac{B}{h} \tag{6}$$

The speed of sound through a liquid, c is related to the density, ρ and bulk modulus by:

$$c = \sqrt{\frac{B}{\rho}} \tag{7}$$

Combining (6) and (7) gives the stiffness of a liquid layer in terms of it acoustic properties:

$$K = \frac{\rho c^2}{h} \tag{8}$$

2.3. Mass and Damping at the Interface

A more complete model of the interface incorporates its mass and damping behaviour. Baik and Thompson (1985) incorporated the effects of mass, *m* (per unit area) of the interface to give the result:

$$R = \frac{(z_1 - z_2)\left(K - \frac{m\omega^2}{4}\right) + i\omega(z_1 z_2 - Km)}{(z_1 + z_2)\left(K - \frac{m\omega^2}{4}\right) + i\omega(z_1 z_2 + Km)} \tag{9}$$

For most tribological interfaces the mass is low (i.e. air gaps and a thin film of oil), so the prediction of equations (9) and (3) are very similar (Baik and Thompson 1985, Margetan et al. 1992). They become more important at high frequency or when the interface is made up of a layer significantly denser than the surrounding media.

Krolikowski et al. (1989) incorporated stiffness and damping (defined by a damping coefficient, η) to give:

$$R = \frac{(z_1 - z_2)(K + i\eta\omega) + i\omega(z_1 z_2)}{(z_1 + z_2)(K + i\eta\omega) + i\omega(z_1 z_2)} \tag{10}$$

It should also be noted that the damping mentioned here is not the same as the squeeze film type damping that an oscillating lubricated contact can cause. Here the wavelength is large compared with the thickness so there is no lateral flow of the lubricant in the contact. Any damping is just that which the lubricant can afford by confined contraction and expansion. This is thought to be small compared with stiffness effects. In most work therefore (Baik and Thompson 1985, Nagy and Adler 1991, Nagy 1992, Drinkwater and Cawley 1997, Lavrentyev and Rokhlin 1998, Baltazar et al. 2002) the basic spring model has been found to adequately describe experimental measurements of the reflection at an interface.

2.4. Continuum Model of Interface Response

Several authors [Hosten, 1991, Kinra et al, 1994, Pialucha and Cawley, 1994] have described numerical continuum models of a multi-layered system response to ultrasonic waves. Based on continuity of stress and strain at each boundary in the multi-layered system, these models can be used to predict the reflection and transmission of plane waves through a given system.

Figure 3 shows a continuum model prediction of the reflection coefficient spectrum for 0.1, 1.0, 15 and 20 μm thickness mineral oil layers between two steel half spaces. This is essentially the *impulse response function* of the system, i.e. it gives the response of the system for an incident wave of unit amplitude. In Figure 3 resonant frequencies are seen as sharp minima in the reflection coefficient spectrum. At frequencies below the resonant frequency the continuum model approach agrees with the spring model.

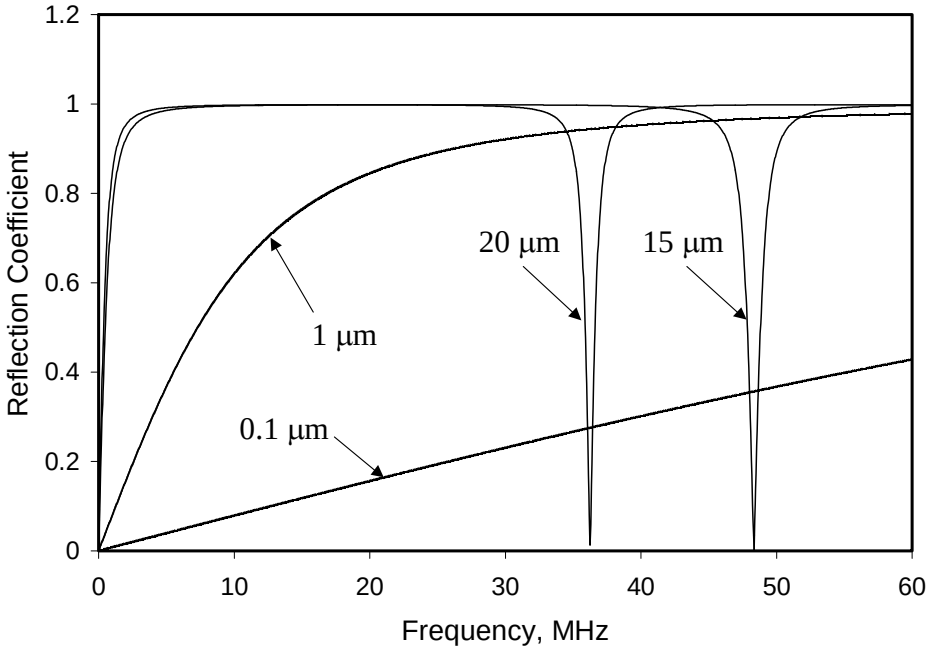

Figure 3. Continuum model predictions of the reflection coefficient spectrum from a layer of mineral oil between two steel elements (using the model of Pialucha and Cawley 1994).

Pialucha and Cawley [1994] used a continuum model approach to show that the resonant frequencies of an embedded layer are related to its thickness, *h*, and acoustic properties by;

$$h = \frac{cm}{2 f_m} \tag{11}$$

where, *c* is the speed of sound in the lubricant layer, *m* is the mode number of the resonant frequency and f_m is the resonant frequency (in Hz) of the m^{th} mode.

The application of such a continuum based model of the multi-layer system can be useful where there is more than one layer present. Many bearing components have a special treated surface layer (either a coating or a modified layer). Depending on the difference in acoustic properties between the layer and the substrate, this extra interface can also cause ultrasonic reflection. Generally for modified surface layers (for example case hardening) there is minimal reflection at the layer substrate interface. However, for a soft or hard coating there can be significant reflection. If the coating is thick then it is possible that the reflection can be separated spatially from the measured reflection from the interface. But thin coatings may disrupt this required signal. These must be treated on a case by case basis.

2.5. Reflection from Dry Interfaces

The spring model approach provides a method for interrogating tribological contacts. The measurement of reflection can be readily related to the stiffness of the interface. This is useful qualitatively as stiffer interfaces indicate a more conformal contact or a thinner oil film.

For contacts made up of surfaces machined with standard engineering finishes (grinding, polishing, turning etc) the stiffness of the interface is such that it can be measured using conventional ultrasonic frequencies. The spring model describes the ultrasonic response well.

This was demonstrated by Drinkwater et al (1996) for a range of rough surface contacts under load. The reflection coefficient is frequency dependent (figure 4a) whilst the stiffness, as predicted by the spring model (equation 2), is frequency independent (figure 4b).

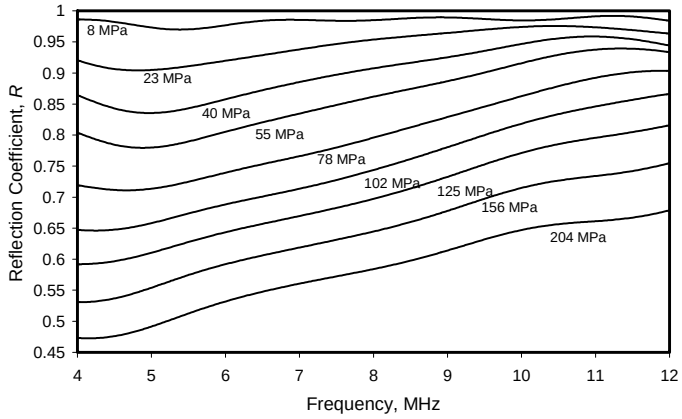

(a)

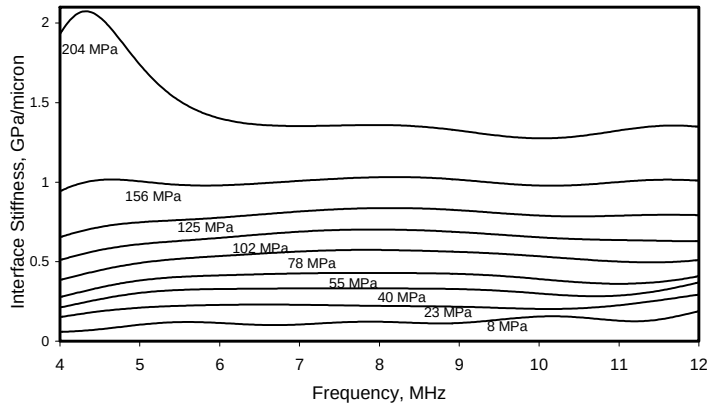

(b)

Figure 4. Experimental reflection measurements from a rough surface contact; (a) the frequency dependence of ultrasonic reflection and, (b) the independence of stiffness as predicted by a spring model approach. Drinkwater et al. (1996).

2.6. Reflection from Lubricated Interfaces

The same equations that describe the response of a dry interface to ultrasound (i.e. the spring model equation 4) can be used for lubricated interfaces. The stiffness of the oil film (equation 8) is used in place of the stiffness of the dry interface. Dwyer-Joyce et al (2002) demonstrated that this relationship holds for thin oil films where the wavelength of ultrasound is greater than the film thickness.

The thickness of most lubricant films (0.1 to 100μm) is in the region such that the stiffness falls within that measurable by conventional ultrasonic test frequencies (below 50 MHz). With thicker hydrodynamic oil films (above ~20μm) resonances occur in the reflection spectrum (as shown in figure 3 above). The location of these resonant frequencies (where the amplitude has been completely transmitted) provides an alternative means of measuring film thickness.

Figure 5 shows measured reflection spectrum obtained from a static oil film created by using thin shims to separate steel gauge blocks (Dwyer-Joyce et al 2002). The reflection is

frequency dependent (figure 7a), but the film thickness determined via the spring model is frequency independent (figure 5b). Note that as the reflection tends to unity (the curve corresponding to 15.9 and 19.5 μm films) the spring model becomes unstable and the predicted film thickness is variable.

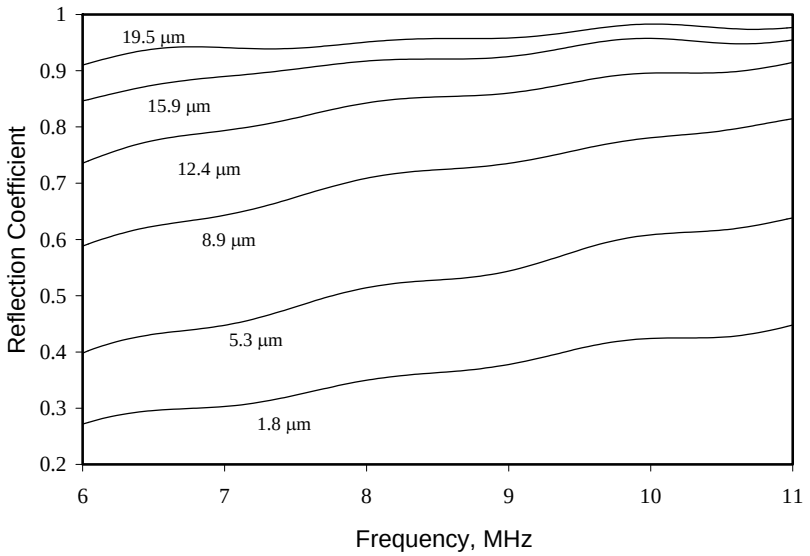

(a)

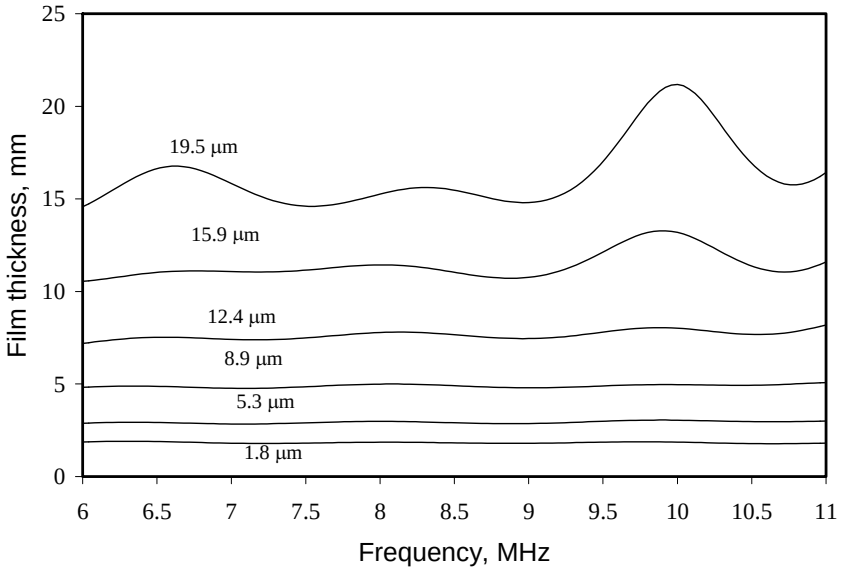

(b)

Figure 5. Measured reflection coefficient spectra for a range of fluid film thickness using a 10 MHz centre frequency transducer; (a) reflection coefficient spectra, and (b) film thickness against frequency. Dwyer-Joyce et al. (2002).

For a thicker film measured at higher frequency (figure 6) resonances occur in the reflection spectrum. The film thickness can then be determined from the location of these resonant frequencies (using equation 11).

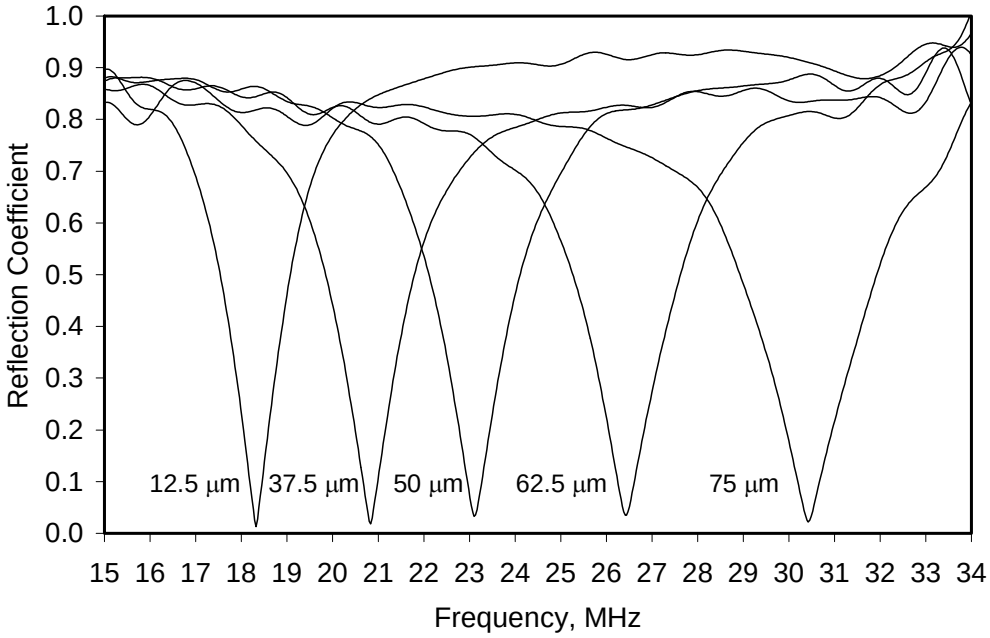

Figure 6. Measured reflection coefficient spectra for a range of fluid film thickness using a 25 MHz centre frequency transducer. Dwyer-Joyce et al. (2002).

2.7. Interface Response to Other Wave Forms

Most work on tribological contacts has been performed using bulk longitudinal waves. The spring model analysis (and continuum model approach) is equally valid for bulk shear waves. The speed of sound in shear is used and the stiffness of the interface is that in the direction tangential to the interface (i.e. the rate of change of tractive force with lateral displacement).

The simultaneous use of shear and longitudinal waves in solid/solid contacts has attracted some interest. Nagy (1992) examined rough surface contacts and so-called kissing bonds (with a finite normal stiffness but reduced shear stiffness). He used a normal and shear rough surface contact model (Yoshioka and Scholz 1989a and 1989b) to deduce the ratio of shear to normal stiffness (which is a function of Poisson's ratio only and thus independent of contact pressure); which successfully compared with experimental predictions. Krolikowski and Szczepek (1993) performed similar experiments and again showed that the stiffness ratio was approximately constant with contact pressure. Baltazar et al (2002) introduced a model that allowed asperity contacts to be oblique (so that the stiffness ratio depends on the contact angle). They also observed an approximately constant stiffness ratio.

When an ultrasonic wave reflects from an incomplete interface there is a phase shift between incident and reflected waves. For the spring model analysis of identical materials the phase shift, ϕ, of the reflected wave is obtained from equation (2) (setting $z_1=z_2=z$):

$$\phi = \pi + \arctan\left(\frac{2K}{\omega z}\right) \tag{12}$$

Again the result depends on the stiffness of the interface. Krolikowski and Szczepek (1992) measured this phase shift from rough surface contacts of both steel and quartz and showed its dependence on contact pressure.

The shear stiffness, K_T, of a thin layer of fluid is a function of its kinematic viscosity, υ, density, the layer thickness, and frequency according to (Nagy 1992):

$$K_T = \frac{i\omega\nu\rho}{h} \tag{13}$$

For most lubricants this stiffness is very low so the wave will be virtually all reflected at the interface. However, some highly viscous liquids (for example molasses which is used as a shear transducer couplant) can transmit some ultrasonic shear waves.

There are other wave forms commonly used in non-destructive testing, such as guided Lamb or Raleigh waves, but these have not been widely used in the study of tribological interfaces.

A recent exception is the work of Drinkwater et al. (2003) who generated guided waves in a flat plate (Lamb waves) and studied their attenuation when an elastomeric block was pressed onto the plate. Attenuation of the wave is caused by transmission through the interface into the block. In the paper a spring type model is used to predict this transmission; which depends on both the longitudinal and shear stiffness of the interface. In an experimental arrangement the stiffness of the interface was deduced both from Lamb wave (anti-symmetric and symmetric orders A_0 and S_0) attenuation and from bulk longitudinal wave reflection. Figure 7 shows the results; reasonable agreement was achieved between the two methods for determining stiffness.

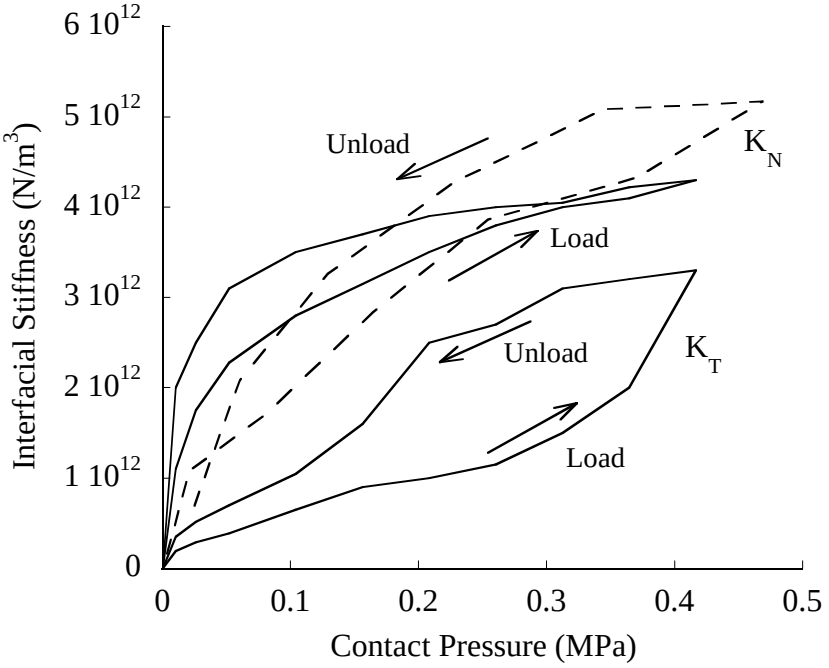

Figure 7. The normal (K_N) and shear (K_T) stiffness of an elastomer/glass interface deduced from measurements of Lamb wave attenuation (solid line) and bulk wave reflection (dotted line). Drinkwater et al (2003).

It is also interesting to note the hysteresis present during the loading cycle; (as with the data shown in figure 16) this is attributed to adhesion at the interface.

2.8. Other Ultrasonic Response Effects at an Interface

One of the assumptions of the spring model is that the wavelength is large compared to the

size of the ‘gaps’ in rough contact (the low frequency regime). When this is not the case and the surfaces are very rough or there are large voids at an interface, then these inhomogenaities will cause oblique scattering of a sound wave. Generally the nature of tribological interfaces found in engineering practice, when investigated with conventional ultrasonic frequencies (less than ~50 MHz), is such that scattering effects are not observed. Margetan et al (1992) carried out experiments to study high frequency reflection from a range of model interfaces. Figure 8 shows a plot of reflection coefficient recorded at an interface consisting of an array of cylindrical voids in an iron block (void diameter 0.36mm and spacing 1.54mm). The results demonstrate that the spring model agrees well for low frequencies; but a scattering model is required to predict higher frequency response. In these experiments, the void size is very much larger than would be expected in a rough surface interface; so the frequency at which the spring model starts to become invalid is much lower.

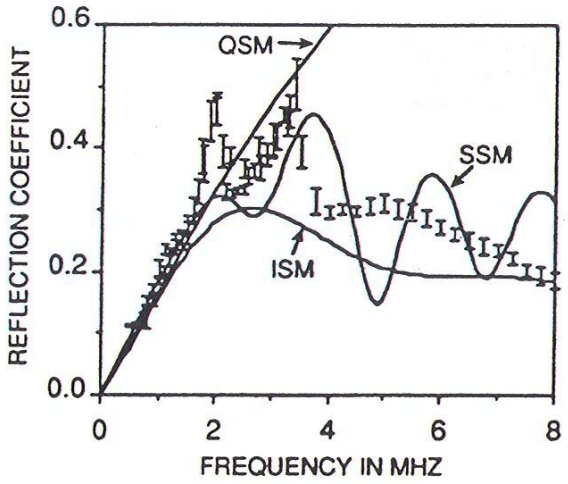

Figure 8. Reflection at an artificial interface consisting of machined cylindrical voids. At low frequency the reflection agrees with a quasi-static spring model (QSM). At higher frequencies an independent scattering model (ISM) or secondary ray scattering model (SSM) must be used.

A further phenomenon that occurs when an ultrasonic wave strikes an incomplete interface, is the generation of higher order harmonics. A change in pressure at the interface (by the passage of a wave) causes a change in the asperity configuration; this non-linear mechanical response causes so called acoustic non-linearity. Investigators (Buck et al. 1978, Solodov 1998) have observed the presence of a second order reflection (occurring at twice the frequency of the incident pulse). Biwa (2004) showed that the amplitude of the reflected second order harmonic is a function of both the interface stiffness and the second order stiffness (i.e. d^2p_{nom}/du^2). As yet, measurements of second order reflections have not been used to study contact conditions in tribological interfaces.

2.9. The Generation and Propagation of Ultrasonic Waves

Figure 9 shows a typical apparatus for the generation and measurement of ultrasonic waves. A pulser/receiver unit is used to generate a series of short duration voltage pulses. These are used to excite the piezo-electric transducer. An oscilloscope or PC digitiser card is used to capture and record the transducer signal. This is then passed to a PC for processing.

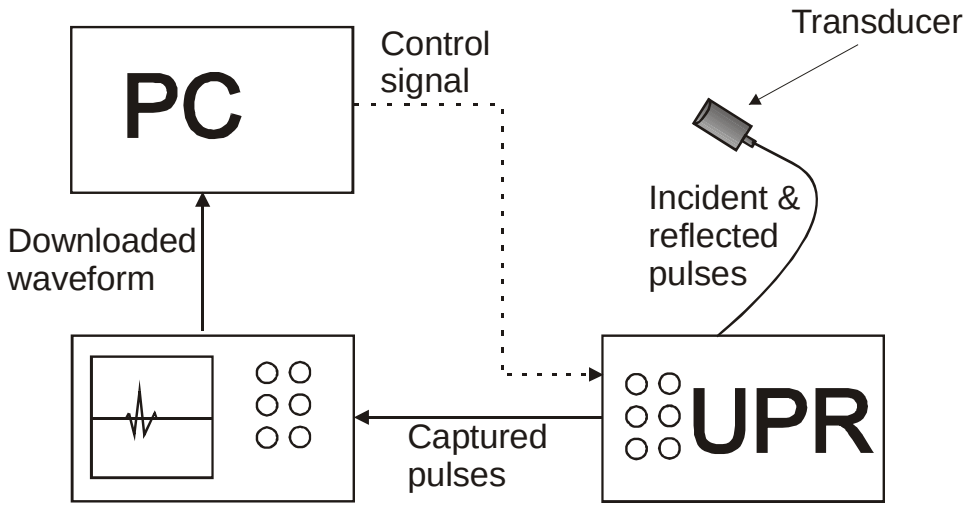

Figure 9. Schematic diagram of typical apparatus for generation and processing of ultrasonic signals. The transducer acts in pulse-echo mode – both sending and receiving pulses.

In early studies the transducers have been bare piezo-electric materials bonded directly to the bearing element. These were pulsed continuously or with relatively long waveforms. More recently conventional ultrasonic NDT type transducers have been used. These consist of a piezo-electric element bonded to a rigid front face (known as a wear plate) and a damping backing material in a protective case. These types of transducer are designed to damp out any reverberation of the crystal after pulsing. This means that short duration pulses can be generated. These also have the advantage of being able to generate a wide band of output frequencies. This gives the possibility of measuring frequency dependence in reflected signals.

Three generic types of transducer are commonly used and are shown schematically in figure 10. Longitudinal transducers generate waves where the direction of oscillation is parallel to the direction of propagation. These can be directly coupled to the specimen using an adhesive or gel (figure 10a), or bonded to a focusing lens and used immersed in a liquid bath (figure 10c). Shear transducers generate waves where the vibration is transverse to the direction of propagation (figure 10b). Shear waves cannot propagate through liquids and so are not useful for measuring oil films (other than the presence or absence of a film).

The transducer frequency must be selected to match the interface being measured, such that a measurable reflection coefficient is expected. If the frequency is too low, for a given interface stiffness, then R tends to zero, if it is too high then R tends to unity. In both cases as the asymptote is reached the signal noise introduces large errors. For rough surface contacts frequencies in the range 200kHz (Kendall and Tabor 1971) up to 90 MHz (Krolikowski et al. 1989) have been used. Above around 50MHz the equipment starts becoming costly and also attenuation in the specimen bulk starts to become more of a problem.

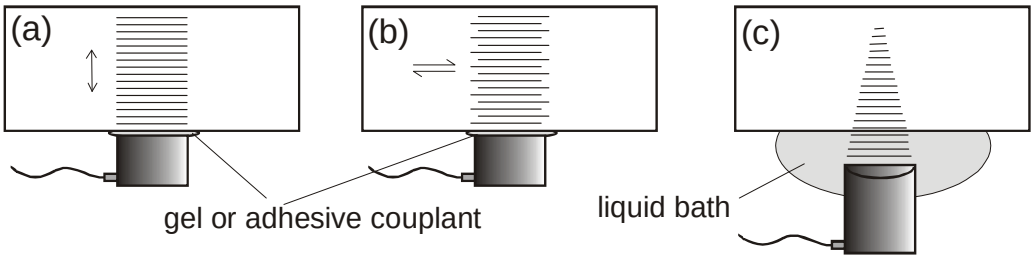

Figure 10. Schematic of three types of transducers used for studying tribological interfaces (a) longitudinal contact, (b) shear, and (c) longitudinal focusing.

3. The Measurement of Dry Contacts

When two nominally flat surfaces are pressed together the contact is made up of asperity contacts and air gaps. An ultrasonic wave will therefore be partially reflected and can potentially be used to determine the stiffness of the contact. Progress has been made by authors from both NDT and Tribology communities. The former, have been concerned with a better understanding of how structural cracks reflect ultrasound, whereas the latter are more concerned with the behaviour of a rough contact.

3.1. Normal Contact and Rough Surface Contact Models

The earliest work on the use of ultrasound to study rough contact was that carried out by Masuko and Ito (1969). They carried out reflection experiments using pairs of machined troostite (a silica based mineral used because it exhibited low acoustic scattering). They showed that rough interfaces reflected less of the wave amplitude than smooth interfaces and that reflection reduced with increasing contact pressure (see figure 11).

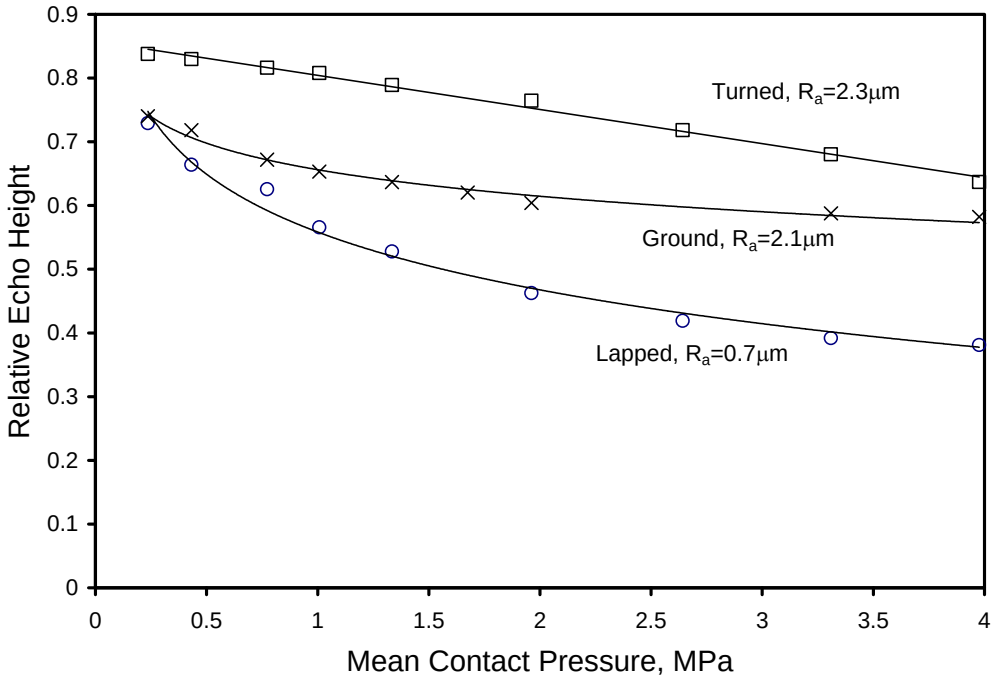

Figure 11. The height of a reflected ultrasonic pulse from contacts between lapped, ground, and turned troostite surfaces (test frequency 5 MHz). Redrawn after Masuko and Ito (1969).

A more extensive set of data, (this time recording the transmitted echo), was presented by Arakawa (1983). A range of ground steel surface pairs were pressed together and the amplitude of the transmitted wave recorded (normalised by the amplitude transmitted through a prefect contact). Figure 12 shows the transmission alongside measured profiles of the two surfaces pressed together. The surface profiles were recorded using a conventional stylus profilometer in a direction perpendicular to the surface lay (it is not clear from the paper but it is likely that there is significant directionality to the surfaces formed). The study also

showed that increasing the ultrasonic frequency increased the amplitude of the reflected signal.

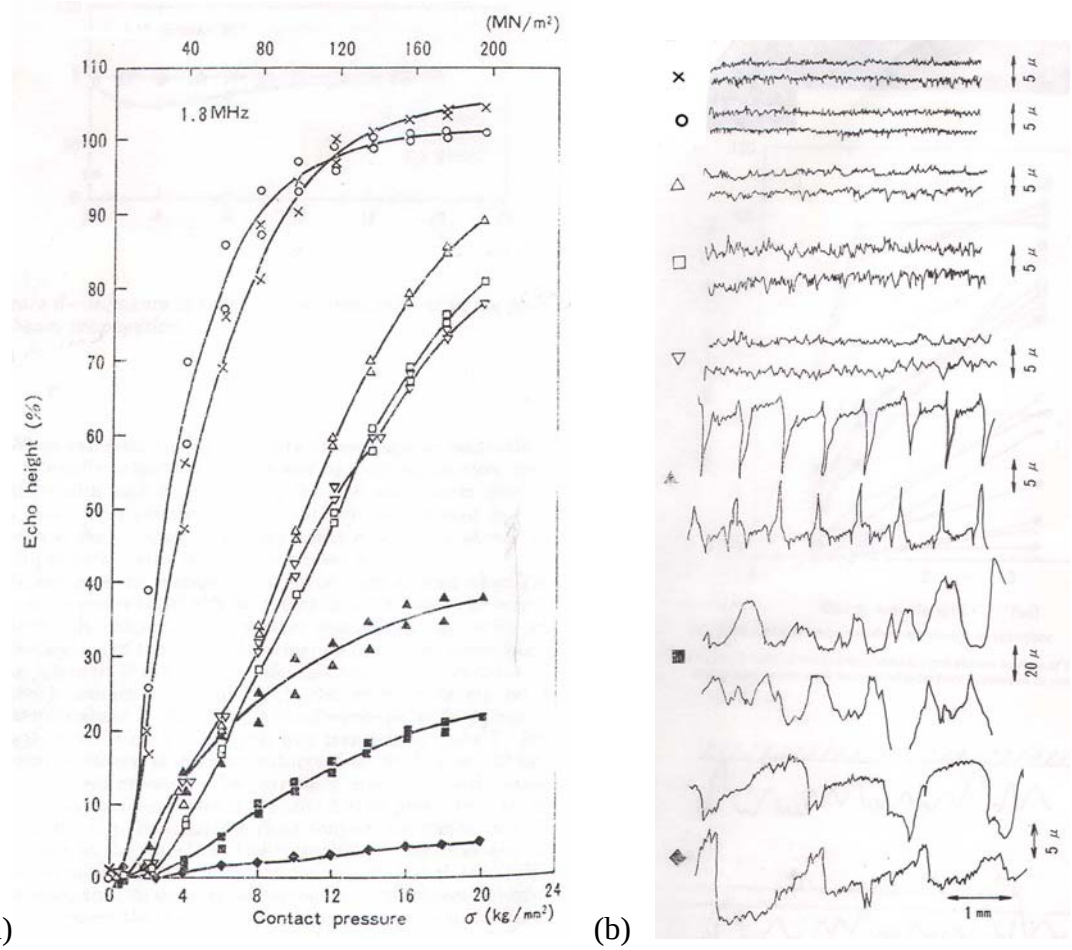

Figure 12. (a) The height of a transmitted ultrasonic pulse through interfaces composed of two rough steel surfaces pressed together (test frequency 1.8 MHz) and (b) the corresponding surface profiles of the specimens recorded perpendicular to the surface lay. Arakawa (1983).

Kendal and Tabor (1971) were the first to analyse ultrasonic reflection behaviour in terms of asperity contact and stiffness. They studied the transmission through a point Hertz contact. Figure 13 shows the stiffness of the contact as it varies with applied load. The real area of contact is somewhat less than that predicted by Hertz and so the stiffness is lower. In elastic contact the expected relationship between stiffness and load is $K \propto p_{nom}^{1/3}$. If the deflection is plastic then an increase in load causes an increase in area but not contact pressure so $K \propto p_{nom}^{1/2}$. The data of Kendall and Tabor followed more closely the square root relationship.

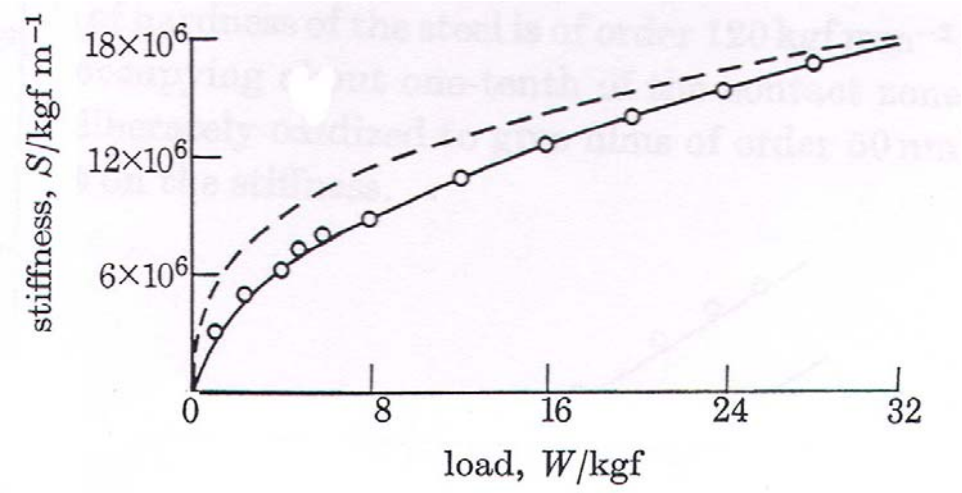

Figure 13. The stiffness of a crossed cylinder contact deduced from ultrasonic experiments. The dotted line is the prediction based on a Hertzian elastic contact. Kendal and Tabor (1971).

Krolikowski and Szczepek (1991) pressed hardened bearing steel platens together and measured the transmission of ultrasound through the interface with increasing pressure (figure 14). The contact stiffness was then determined from a spring damper model (equation 10); shown as figure 15.

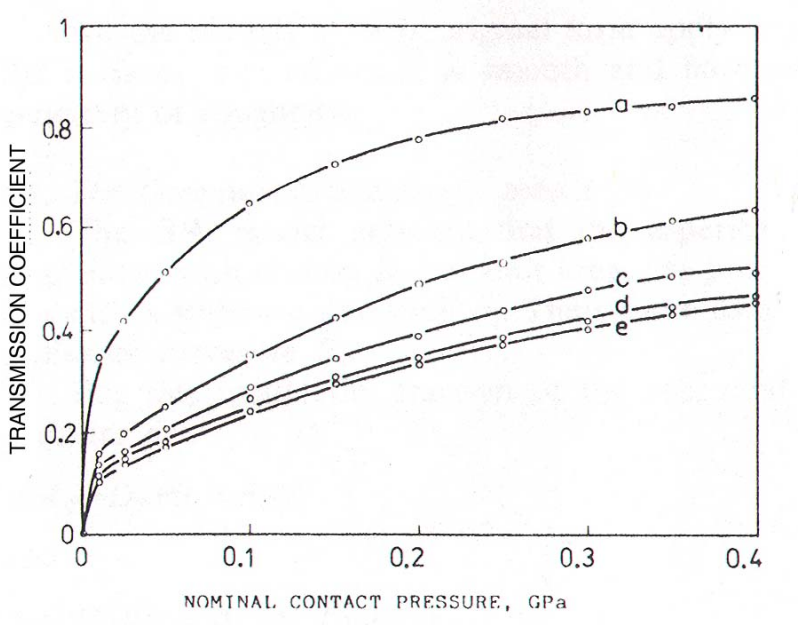

Figure 14. Transmission of ultrasound through a bearing steel contact; showing the effect of contact pressure and measurement frequency. Krolikowski and Szczepek (1991)

There are a variety of contact models that can be used to predict interface behaviour, typically they relate the approach of the surfaces, *u* to the nominal contact pressure, and real area of contact. The relationship between pressure and approach can be differentiated to give stiffness. Krolikowski and Szczepek (1991) determined the interface stiffness using three published statistical models of elastic surface contact; these are over plotted on figure 15.

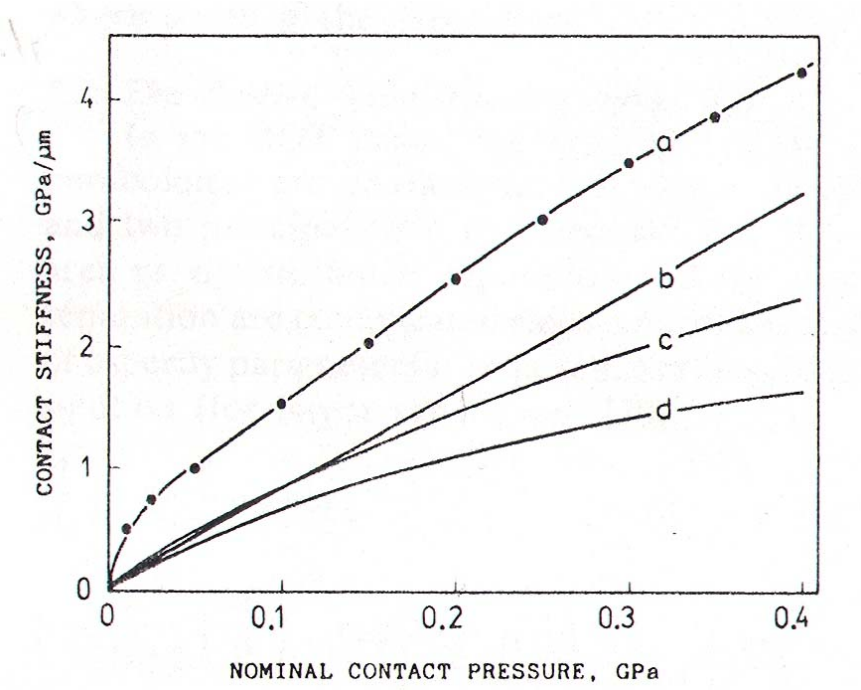

Figure 15. The stiffness of a bearing steel contact determined (a) ultrasonically, and compared against the rough surface contact models of (b) Bush et al (1975), (c) Whitehouse and Archard (1970), and (d) Greenwood and Williamson (1966). Krolikowski and Szczepek (1991)

The agreement between the measurements and predictions is qualitative rather than quantitative. Similar comparisons have been explored by Drinkwater et al (1996) for a range of surface roughness specimens but this time using the numerical contact model of Webster and Sayles (1986) based on measured surface profiles in elastic contact. Again the agreement is modest with the ultrasonic measurements leading to stiffer surfaces than predicted. A possible explanation lies in the fractal nature of rough surfaces. It is possible that the scale on which the ultrasound is sensitive is larger than that on which the surface-measuring device is recording the roughness. Essentially the mechanism of ultrasonic reflection does not see the finer asperities recorded by the profilometer.

3.2. Repeated Contacts

The first loading of the contact takes place plastically. When the contact is unloaded the asperities have been flattened to a more conformal shape and the interface is stiffer. The ultrasonic reflection and interface stiffness changes during this process are presented in Dwyer-Joyce et al. (2001). Figure 16 shows a plot of stiffness and contact pressure for a series of loading cycles. The first cycle is largely plastic whilst the subsequent reloading occurs largely elastically. However the successive loading cycles do show a constant hysteretic behaviour; this was attributed to irreversible adhesion at the interface.

Figure 17 shows a plot of a similar series of loading cycles but this time occurring at increasing end loads. The loading lines are contiguous whilst unloads are virtually elastic.

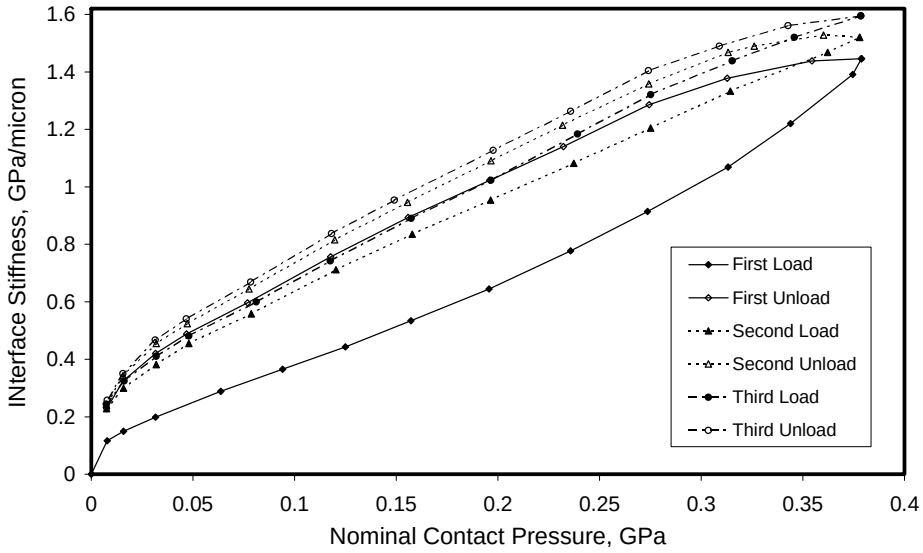

Figure 16. Cycles of loading on a rough surface contact. Ultrasonically measured stiffness is shown varying against contact pressure (Dwyer-Joyce et al 2001).

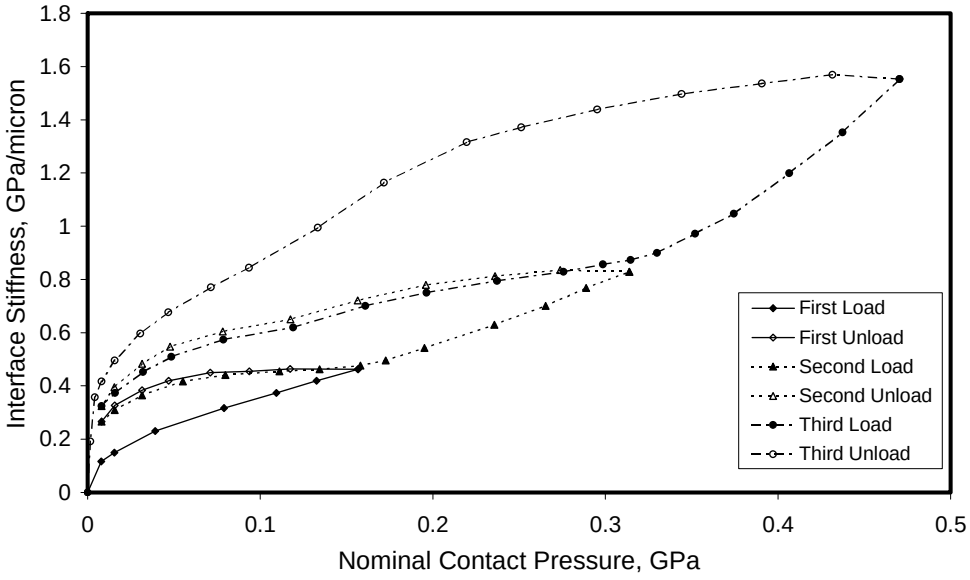

Figure 17. Cycles of loading on a rough surface contact; the end load is increased for each cycle. Ultrasonically measured stiffness is shown varying against contact pressure (Dwyer-Joyce et al 2001).

3.3. Determination of Real Area of Contact

In the literature, there is some disagreement as to how the real area of contact might be deduced from ultrasonic reflection or transmission measurements. Kendall and Tabor (1971) rightly point out that, the stiffness of the interface is a function of the number and size as well as the distribution of asperity contact regions. So it is therefore not possible to determine real contact area uniquely from stiffness. In figure 18 both contacts have the same real area of contact. Where the isolated of contact are closely packed (figure 18b) the stiffness is reduced

(because the load on one contact region causes the deflection of the nearby regions). Where the contact regions are widely distributed (figure 18a) the interface is stiffer. Kendall and Tabor (1971) carried out some simple experiments pressing cylindrical disks into a soft rubber block and showed that only when the contact regions are around three diameters apart (i.e. separated by a distance of around 6*a*) does the empty space between the contacts have any effect. This corresponds to a contact area ratio of about 10%; so only when the area ratio is less than this can the individual contact regions be considered as acting independently.

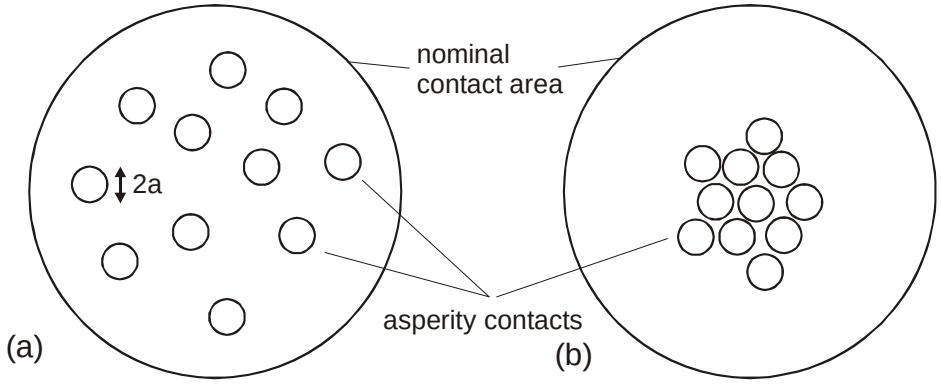

Figure 18. (a) Distributed, and (b) closely packed regions of asperity contact within a rough surface interface.

If the contacts are assumed to be distributed then the stiffness of the interface can be determined from:

$$K = \eta\gamma E^* \bar{a} \tag{14}$$

where η is the number of asperity peaks per unit area, $\bar{a}$ is the average radius of a contact region, E^* is the reduced modulus, and γ is a constant which depends on the pressure distribution across the contact region (being $\pi/2$ for uniform pressure and 2 for a Hertzian contact). Then for fully plastic contact regions the ratio of real area to nominal of contact is:

$$\frac{A_r}{A_{nom}} = \frac{p_{nom}}{H} = \eta\pi\bar{a}^2 \tag{15}$$

where H is the hardness of the surface.

Dwyer-Joyce et al. (2001) used this simple model to interpret ultrasonic results. The interface stiffness of a rough surface contact was determined for a range of contact pressures. The data was then used in the simultaneous equations (14) and (15) to deduce the size (Figure 19a) and number (figure 19b) of asperity contacts.

The results show that the average size of a contact patch is approximately constant whilst the number of contacts increases linearly with pressure. As the load on a contact increases, the existing contact regions grow in size but more new small areas are formed; the average contact spot remains approximately constant whilst the number of spots increase linearly. This is consistent with the fact that friction coefficient is observed to be independent of load (Amontons' law of friction). For this to be the case then the total real contact area must grow in direct proportion to the load. Since the real contact area is given by the number of contact spots multiplied by the square of their radius, then direct proportionality can only be achieved if the contact size remains constant but the number of contacts grows linearly.

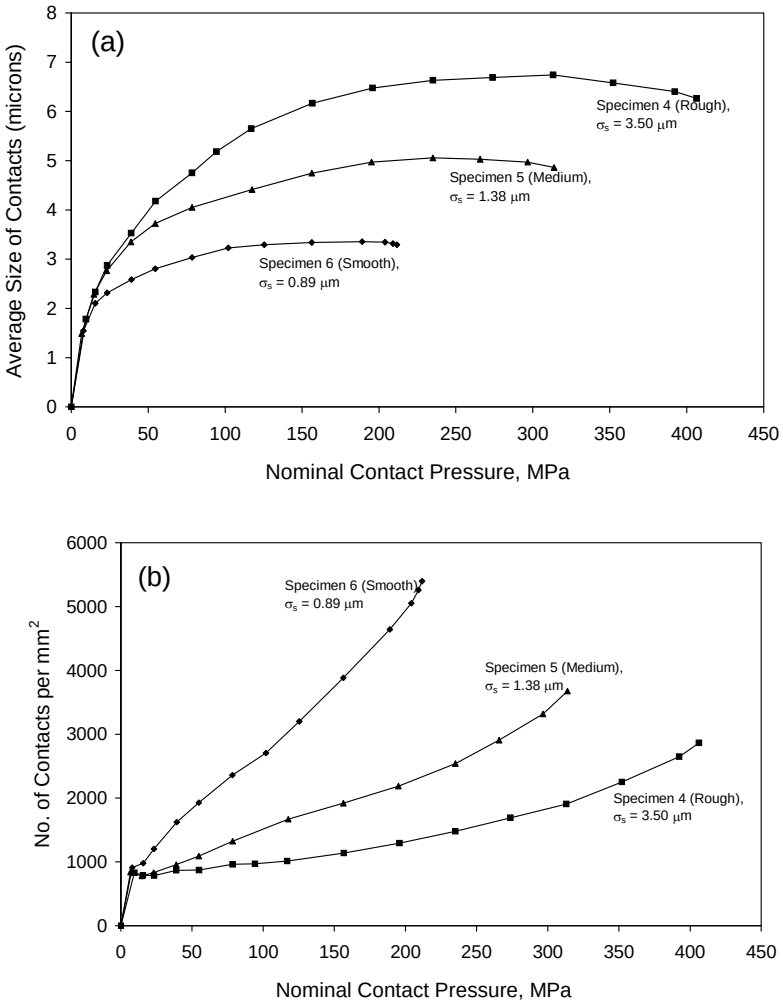

Figure 19 (a) Average size and (b) number of contact regions as deduced from ultrasonic reflection measurements. Dwyer-Joyce et al. (2001).

Polijaniuk and Kaczmarek (1993) suggest that the square of the transmission coefficient (based on wave energy rather than amplitude) is a good measure of real area of contact. They measure the variation of reflection with pressure for 32 pairs of steel rough surfaces in contact (from R_a ranging from 0.3 to 46 μm). They measured the bearing area ratio of the unloaded surfaces to estimate the residual contact area after elastic unloading. Figure 20 shows that they observed a closely linear correlation between transmission and bearing ratio.

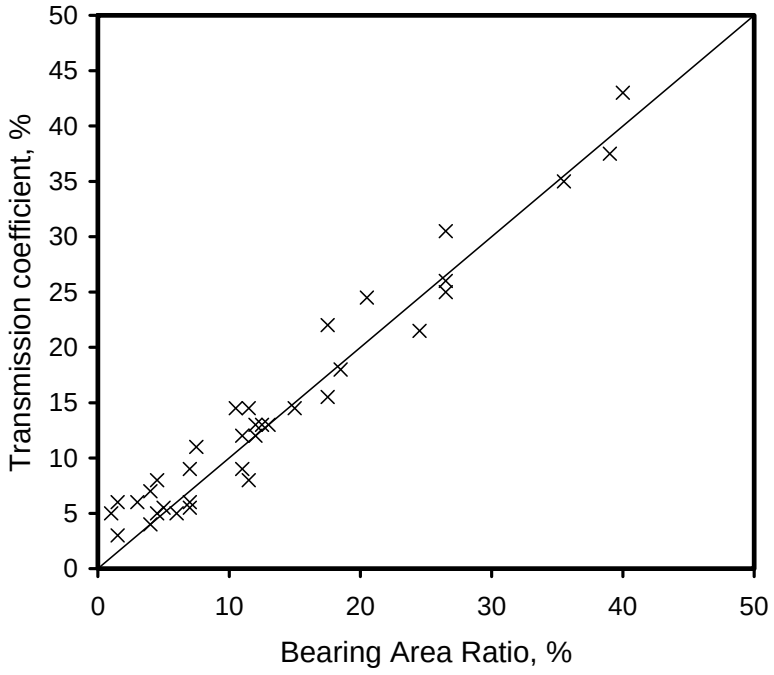

Figure 20. The relationship between transmission coefficient and the bearing area ratio for loaded steel surfaces with a range of roughnesses. Redrawn after Polijaniuk and Kaczmarek (1993)

Krolikowski & Szczepek (1991) use a different approach. They suggest that damping at the interface can be used to determine real area of contact. When the frequency approaches infinity the transmission coefficient reaches a limiting value, T_{min} deduced from equation (10):

$$T_{\min} = \frac{1}{\left(\frac{z}{2\eta}\right)+1} \tag{16}$$

And their assumption is that the real area of contact is equal to the square of this minimum transmission.

$$T_{\min} = \left(\frac{A_r}{A_{nom}}\right)^2 \tag{17}$$

It should be pointed out that in other work (Baik and Thompson 1985, Nagy and Adler 1991, Nagy 1992, Drinkwater and Cawley 1997, Baltazar et al. 2002) the effects of damping were found to be negligible. In the tests where identical materials are pressed together the reflection tends to unity (i.e. $T \rightarrow 0$) with both increasing pressure and increasing frequency. The results are fitted well by a simple stiffness model (without damping terms). However, the work of Krolikowski & Szczepek (1991) is the first to go to such high frequencies (90 MHz) and perhaps at these high frequencies interface damping becomes an issue.

It has been noted (Arakawa 1983, Hodgson et al. 2000) that for the first loading of a rough surface pair, the stiffness is approximately linearly proportional to the nominal pressure ($p_{nom}=cK$). This provides a simple calibration route for maps of contact stiffness (Dwyer-

Joyce and Drinkwater 1998). If the total load on a contact is known then the constant of proportionality can be determined easily ($P=\Sigma\, p_{nom}=c\Sigma K$). Another method is to carry out a completely separate calibration experiment to determine the relationship between K and p_{nom} (Marshall et al 2004b). Specimens have to be cut from the same material with the same contact surface roughness. These are loaded in a hydraulic press and the reflection recorded. The spring model is used to obtain a stiffness that is calibrated against the nominal contact pressure. Clearly the approach will only work for the first loading of two surfaces. The path of the unloading curve will depend on the previous load history. So unless this path completely follows that of the application it is not suitable as a calibration route.

This approach has been used to produce contact pressure maps from simple point contacts and other interface geometries (as shown in §4).

3.4. Sliding Contacts

Little work has been done to study features of sliding contact with ultrasound. The reason for this is probably one of experimental complexity. If wear takes place then the debris particles trapped between the surfaces scatter ultrasound and can significantly change the reflection coefficient. There have been no attempts to date to quantify the effect of debris generation on sound transmission.

Kendal and Tabor (1971) used both glass and steel surfaces in sliding (10^{-3} to 10 mm/s) and measured contact stiffness in the same way as for static surfaces. After a short sliding distance the surfaces become scratched and roughened causing the transmission and hence stiffness to fall. The same experiments were repeated with lead and indium surfaces. In this case the acoustic transmission was seen to increase with sliding. They proposed that the area of contact increased with sliding distance and attributed the observation to junction growth (the size of individual asperity contacts increasing with the application of shear stress during sliding).

Contacts sliding at much higher speeds were investigated by Takeuchi et al (1995) with a pin on disk apparatus. They measured reflection from steel running against PTFE at 250 mm/s. They observed a correlation between friction force and transmission (see figure 21a). As the real area of contact between two surfaces increases so both the friction and the transmission increase. In the study they also scanned the transducer across the sliding contact. In this way they were able to map out reflection and used the correlation between reflection and friction to produce a map of friction across the whole disk surface (see figure 21b). They attributed the spatial variation in friction to local protective oxide films that modified the contact area and friction.

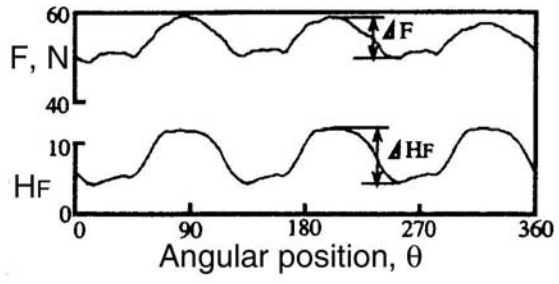

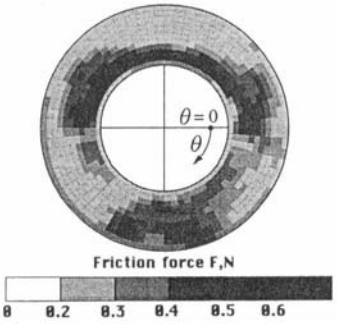

Figure 21 (a) The correlation between friction force (F) and transmitted ultrasound (H_F) for a steel slider on a PTFE disk. A map of transmission has then been used to produce (b) a map of friction force across the test specimen surface. Takeuchi et al (1995).

Surface roughening by wear causes significant change in the reflected ultrasonic pulse. Figure 22a (extracted from Ahn and Kim 2001) shows reflection monitored during a wear test carried out under three different regimes (mild, transitional, and severe). The progress of wear has caused the signal amplitude (and hence reflection coefficient) to drop. As the surfaces become rougher the stiffness reduces and the reflection increases. The reduced amplitude can be correlated with increased friction and wear depth (see figure 22b & c).

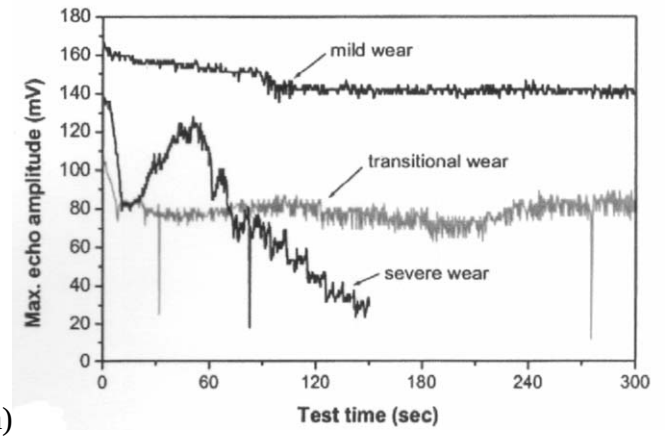

(a)

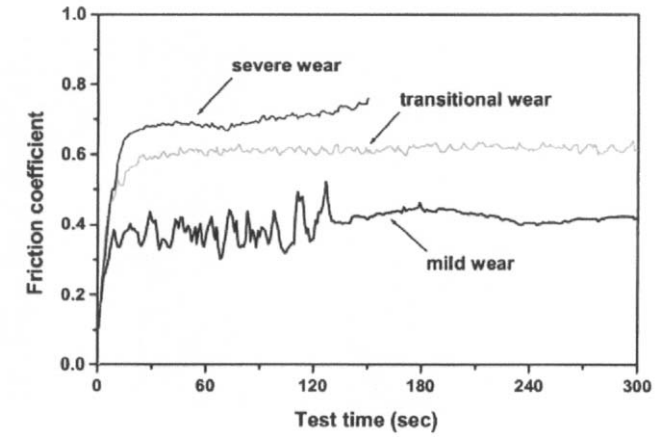

(b)

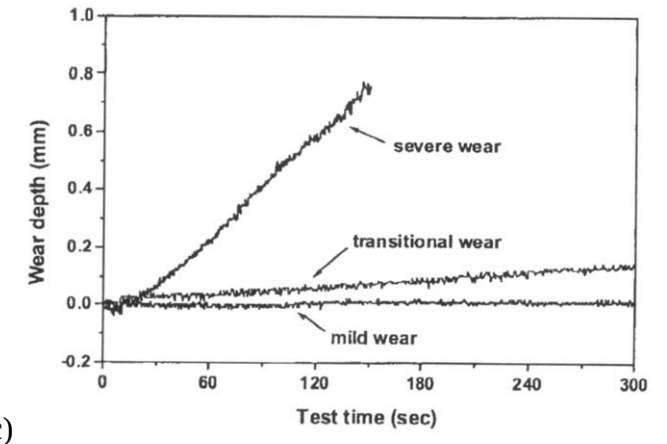

(c)

Figure 22. (a) Ultrasonic reflection from three sliding wearing contacts and the corresponding (b) friction coefficient, and (c) wear depth. Ahn and Kim 2001

Incidentally, these authors monitored the depth of wear using a time of flight method. As material was removed the interface moved closer to the transducer. The time of arrival between the incident and reflected pulses therefore reduces. This reduction provides a suitable method for determining the wear depth. Ultrasound is commonly used as a thickness gauge in this way and has successfully been used to measure depth change due to wear in wear test samples (Long and Rack 1997) and engine liners (Birring and Kwun 1989).

4. Applications to Engineering Components

The techniques described above have been implemented for the analysis of several machine element contacts. Generally this has been driven by a motivation to either, improve the understanding of how the component works to enhance development, or as a tool for condition monitoring. There follows a brief review of some of these applications and an explanation of how ultrasound has been used as a diagnostic tool.

4.1. Mechanical Seals

Mechanical face seals rely on one smooth ring spring loaded against a counterface. The contact is designed to operate with a thin fluid film or with a very light contact. Excessive contact quickly leads to surface damage, wear, and failure. This kind of seal is used extensively in rotating fluid machinery where seal failure can have catastrophic results. The work carried out by Anderson et al (1999, 2000 and 2001) has been to evaluate the use of ultrasound to measure the onset of excessive contact in both gas and liquid seals. Figure 23 shows the positioning of a piezoelectric transducer behind one of the seal faces for reflection measurements. They use both reflection and transmission measurements of shear and longitudinal waves to determine the onset of excessive contact in a seal apparatus for liquids (Anderson et al 2000, 2001) and gases (Anderson et al 1999) respectively. Figure 24 shows a typical result where the amplitude of the reflected wave is compared to the seal leakage rate. When the seals faces are out of contact, in these experiments, the wave is virtually all reflected. As soon as contact occurs the reflection drops and the leakage rate reduces.

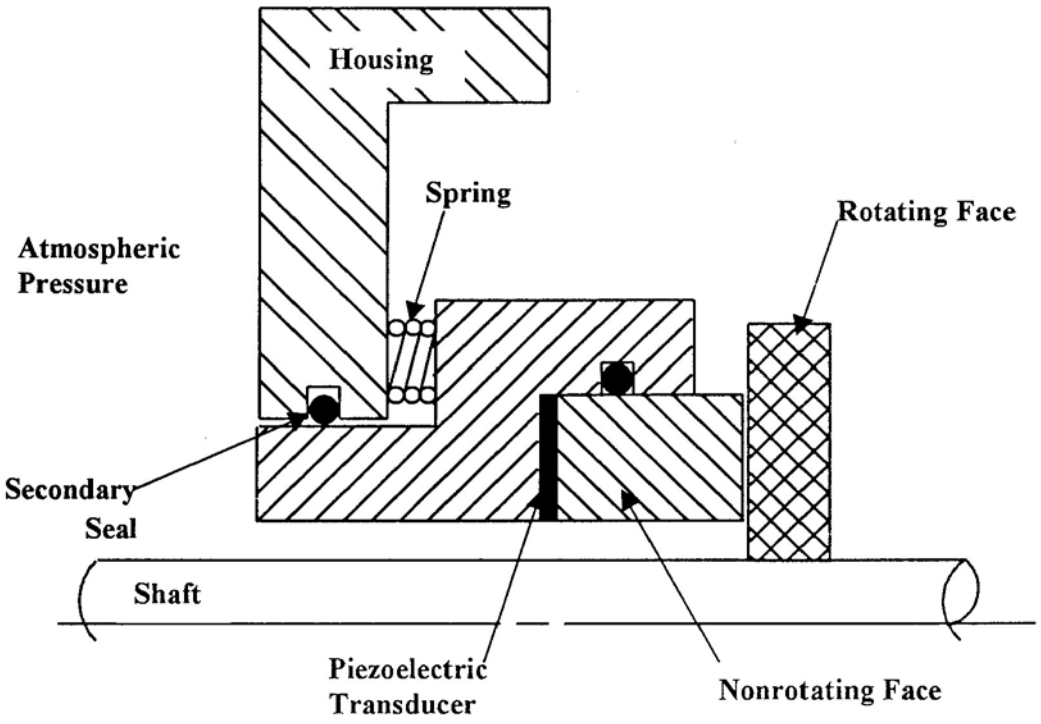

Figure 23. Schematic diagram of the positioning of an ultrasonic sensor in a mechanical seal assembly. Anderson et al (2000).

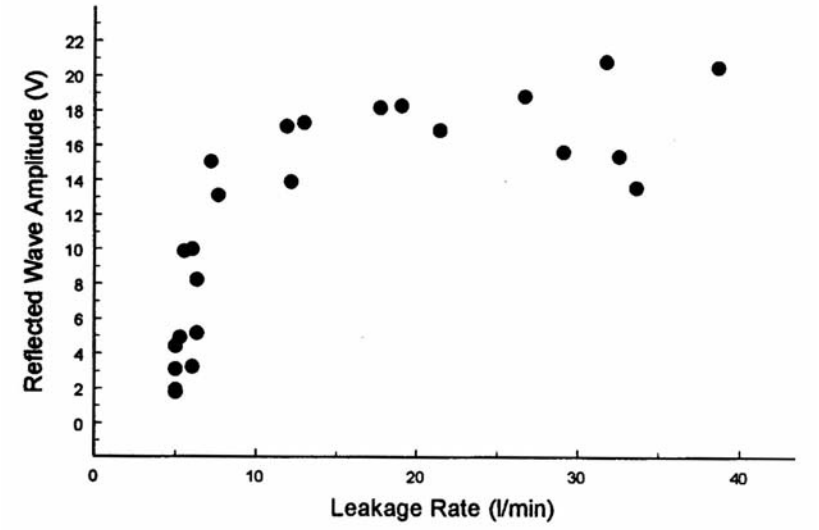

Figure 24. The amplitude of an ultrasonic wave reflected at a mechanical seal contact. When the seal is in contact both reflection and leakage are minimal. Anderson et al (2000).

4.2. Bolted Joints

Contact pressure is an important parameter in determining the fatigue life of a bolted joint. Typically in design guides the bolt tension is modelled as spreading away from the bolt in a cone with an apex angle of 2α. The extent of the contact pressure generated by a tightening bolt has been measured ultrasonically. Ito et al. (1979) performed some spot measurements and used a calibration procedure to determine contact pressure from ultrasonic reflection.

Figure 25 shows the contact pressure variation with radial distance from the bolt axis for two flange contact loads and two surface finishes.

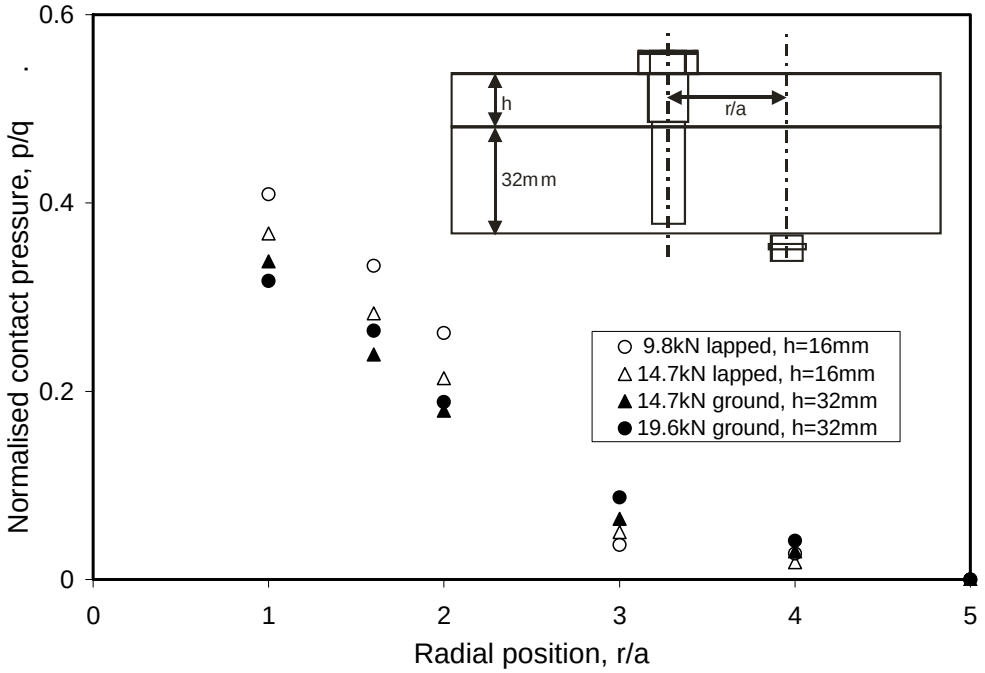

Figure 25. Radial distribution of contact pressure, *p* (normalised by nominal flange pressure, *q*) in a bolted jointed determined from ultrasonic reflection (the radial position, *r* is normalised by the bolt hole radius, *a*). Ito et al. (1979).

More recently maps of the contact pressure in bolted joints have been created (see figure 26) using a similar approach Marshall et al (2004a). In both cases, the ultrasonic results generally show that the measured pressure cone is more widely spread than theoretical predications.

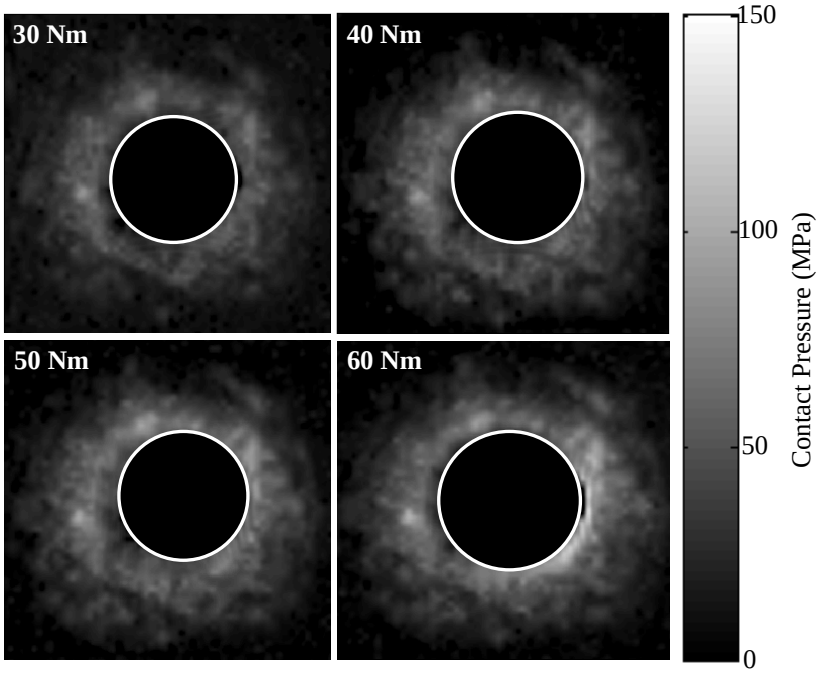

Figure 26. Map of contact pressure in a bolted jointed determined from ultrasonic reflection.

Marshall et al. (2004a).

4.3. Press and Shrink Interference Fits

Interference fits are a common method of joining rotating components (axles and wheels, impellers and shafts etc.). A bush is press or shrunk fit onto a shaft of slightly larger diameter. The interference joint makes an ideal case for ultrasonic study because the contact area is large and relatively flat.

Tsao et al (1984) and Mott and Taszarek (1985) recorded reflections from interference fit interfaces and were able to qualitatively relate low reflected signals to regions of high contact pressure. Lewis et al. (2003) performed scans of model interference fits and used a calibration process to determine contact pressure (an example is shown as figure 27). The stress concentrations at the bush edges are clearly visible. In this work scanning focussing transducers were used. Their spatial resolution is typically ~200μm. So measurements up to this distance from the bush edge can be recorded. In the work several techniques to reduce edge effects were used and also a cavity was incorporated within the fit as a reference point. The authors were also able to ultrasonically image damage that had occurred at a press fit that had galled during assembly.

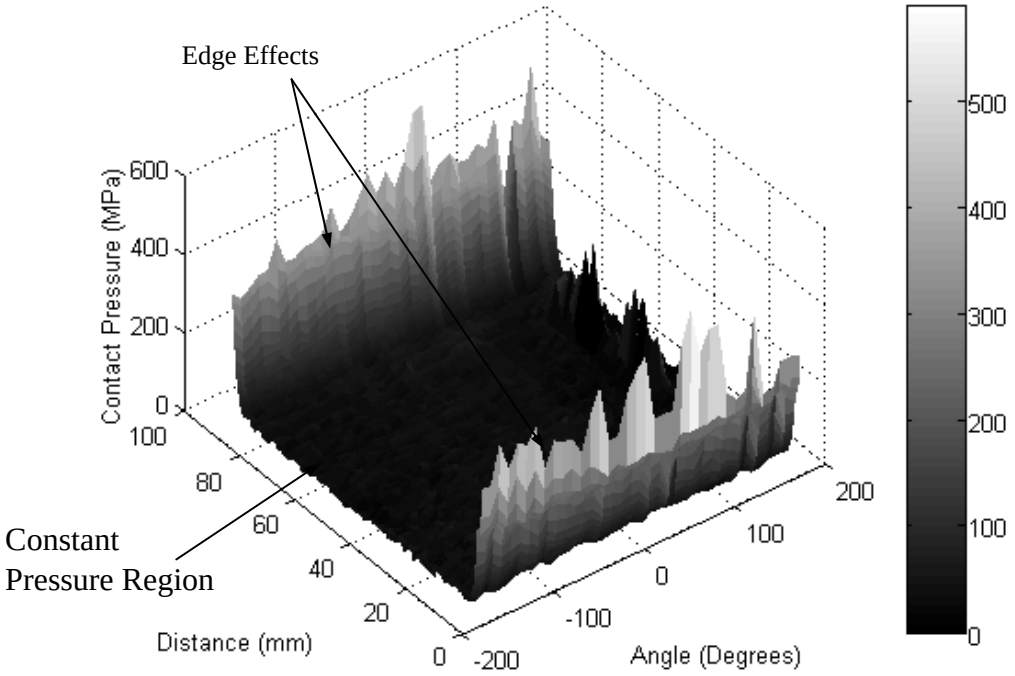

Figure 27. Contact pressure map for an interference fit (50μm on a 50mm bore) deduced from ultrasonic reflection. Lewis et al. (2003).

4.4. Wheel-Rail Contact

Possibly the biggest common concentrated contact occurs between a railway wheel and rail. Pau et al. (2000, 2002, 2003) used a scanning focused transducer to map specimens of wheel and rail loaded together hydraulically. Figure 28 shows their experimental arrangement. Figure 29 shows a series of three maps of ultrasonic reflection recorded at increasing contact load. They used an image processing technique (calibrated using contacts of known size) to determine the nominal area of contact.

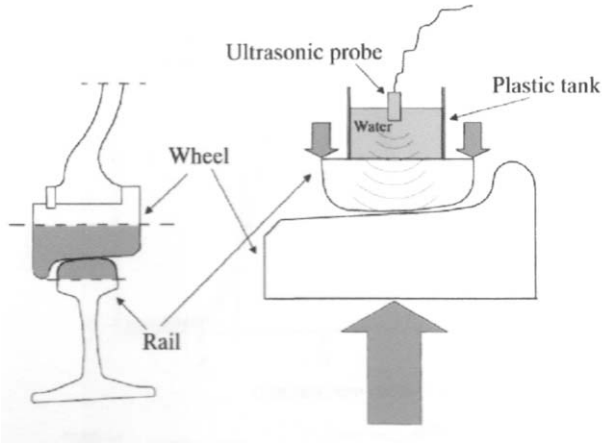

Figure 28. Experimental arrangement for ultrasonic scanning of a wheel rail contact. Pau et al. (2002).

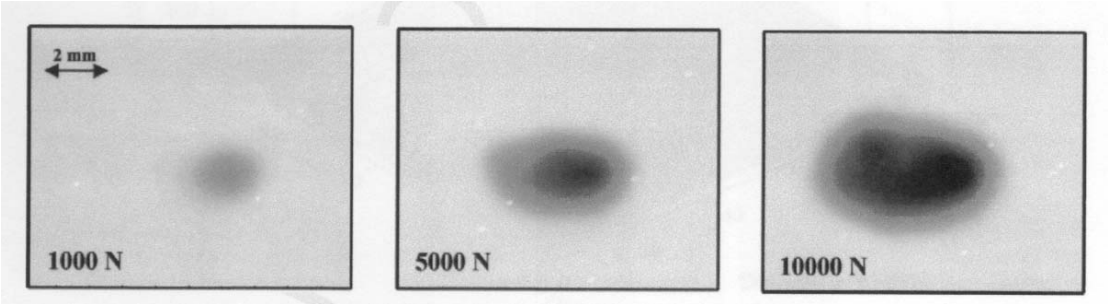

Figure 29. A series of reflection maps recorded at increasing loads on a wheel-rail contact. Pau et al. (2002)

In similar work, Marshall et al (2004c) compared pressure maps with the solutions given by Hertz theory, an elastic numerical model, and an elastic-plastic numerical model (see figure 30). The numerical models used real measured surface profiles from the wheel and rail specimens. The profiles were digitised and numerically overlapped; a matrix equation was set up to relate the surface deflections and the point loads at each node point. An iterative procedure was established to determine a compatible surface deflection profile and contact pressure distribution. Essentially the numerical model incorporates surface roughness and form effects, but still assumes that the contact bodies can be treated as infinite half-spaces.

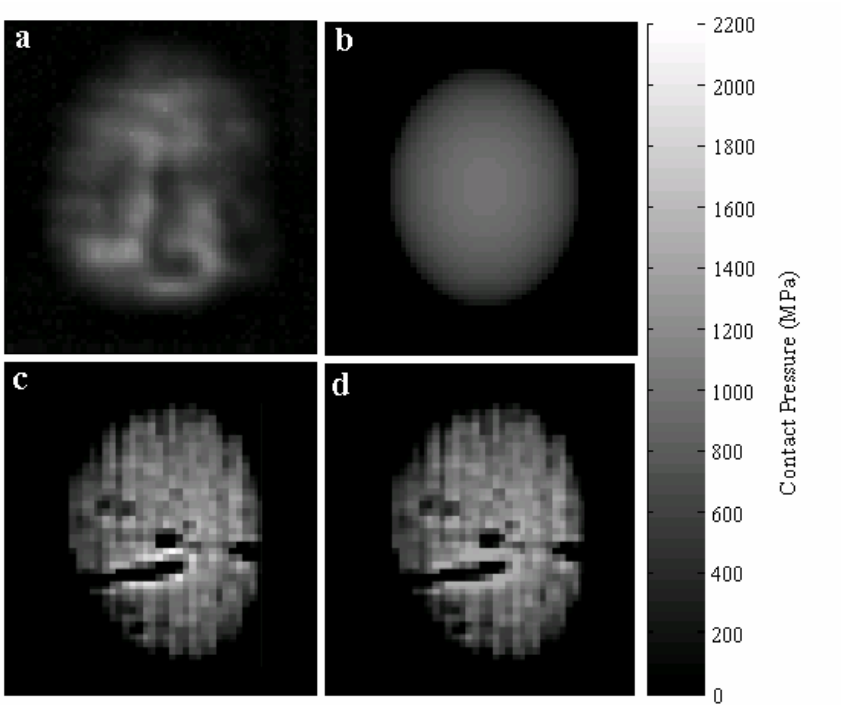

Figure 30. Contact pressure maps for a loaded wheel-rail contact (80kN) (a) ultrasonic measurement; (b) Hertzian prediction; (c) elastic model prediction (d) elastic-plastic model prediction. Marshall et al (2004c)

The spatial resolution of a focusing transducer (in the range 0.1 to 0.4 mm) means that these kinds of measurements are approximations only. The method at this time is also limited to planar contacts; so the simultaneous measurement of head and flange contact would be difficult. A challenge here would be to measure contacts in a operating wheel rail environment (in that case the contact movement would provide one axis of the ‘scan’).

4.5. Open and Closed Cracks

The most commonly studied application of ultrasound to study contacts has been that of structural cracks under compressive stress. The NDT community are concerned that if cracks are loaded, by either applied or residual compression, then they might allow ultrasonic transmission and so be harder to detect. It is not the purpose of this paper to review this large body of work in detail. Many of the approaches are similar to those used in study dry rough contacts. Haines (1980) deduced interface stiffness from statistical models of rough surface contact and compared these with ultrasonic spring model predictions.

In several publications Wooldridge et al. (1979, 1980a, 1980b) showed that the ultrasonic reflection firstly depends on how the crack was grown, since roughness typically correlates with the stress intensity factor. Their experiments showed that the presence of a compressive stress causes the crack reflections to reduce considerably (up to 12dB for a normal incidence signal). The group of Thompson in several papers (Thompson et al 1983, Baik and Thompson 1984, Buck and Thompson 1984) have also studied this problem extensively. They have used models of the interface based on equi-spaced arrays of voids to define ultrasonic response.

4.6. Oil Film Thickness Measurement in Journal and Rolling Element Bearings

Ultrasonic reflection has been used to measure oil films in a journal bearing (Dwyer-Joyce et al. 2004b); figure 31 shows the experimental arrangement. A planar transducer was glued to the outer face of the bush and reflection measurements recorded for a range of loads and speeds. The spring model approach was used to determine the oil film stiffness and hence its thickness. The temperature of both the oil film and the transducers were monitored. The acoustic properties of oil vary slightly with temperature, as does the output of the transducer. Both variations had to be accounted for in the measurements. Results were consistent with predictions of theoretical predictions of film thickness; figure 32 shows the film profile around the bearing circumference.

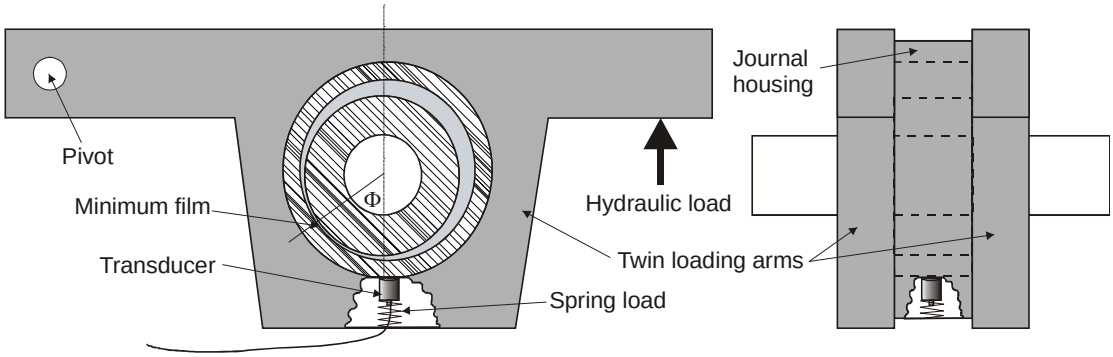

Figure 31. Schematic diagram of apparatus used to measure oil film thickness in a journal bearing. Dwyer-Joyce et al. (2004b).

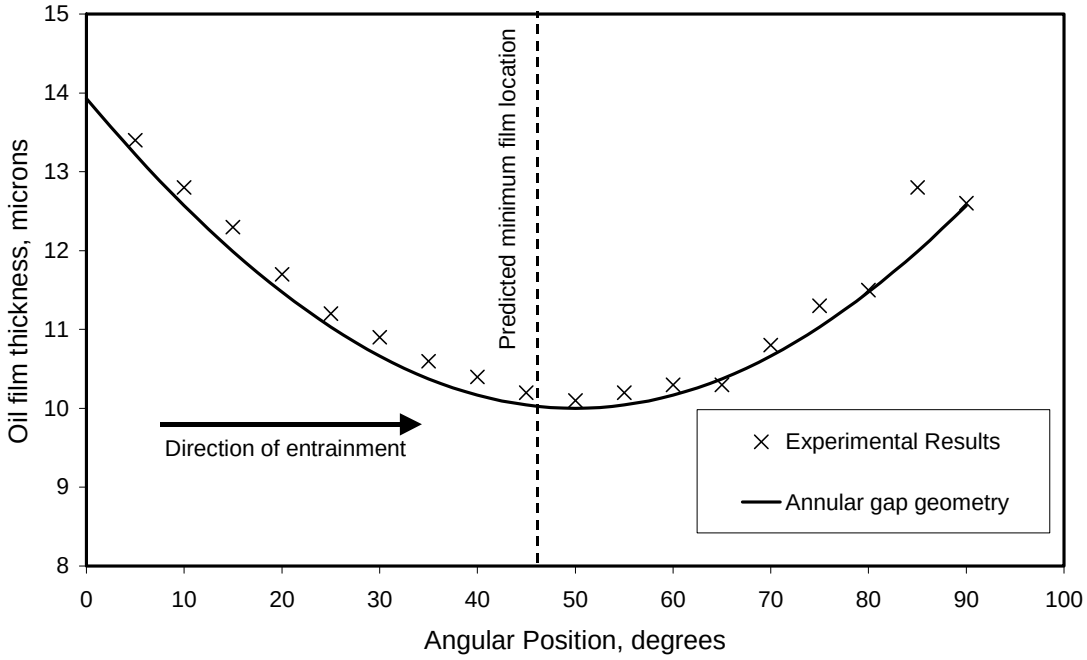

Figure 32. Journal bearing oil film thickness measurements recorded around the circumference of the bush. In the divergent part of the film cavitation occurs leading to a more erratic signal. Dwyer-Joyce et al. (2004b).

Measurements of oil film thickness in an elastohydrodynamic lubricated (EHL) contact are more difficult. The transducer must be focused and positioned accurately with respect to the contact. The analysis is further complicated by the fact that the oil under EHL pressures has an elevated bulk modulus. This needs to be determined before the film thickness can be obtained from reflection measurements. Such a procedure is described in Dwyer-Joyce et al. (2002) for a ball sliding against a flat plate. High frequency transducers (35 MHz and 50 MHz) were used to achieve a small focused spot and film thickness resolution in the sub-micron range. The results from high-pressure viscometer studies were used to estimate the bulk modulus. Figure 33 shows the experimental arrangement and the results compared with theoretical steady state EHL solutions.

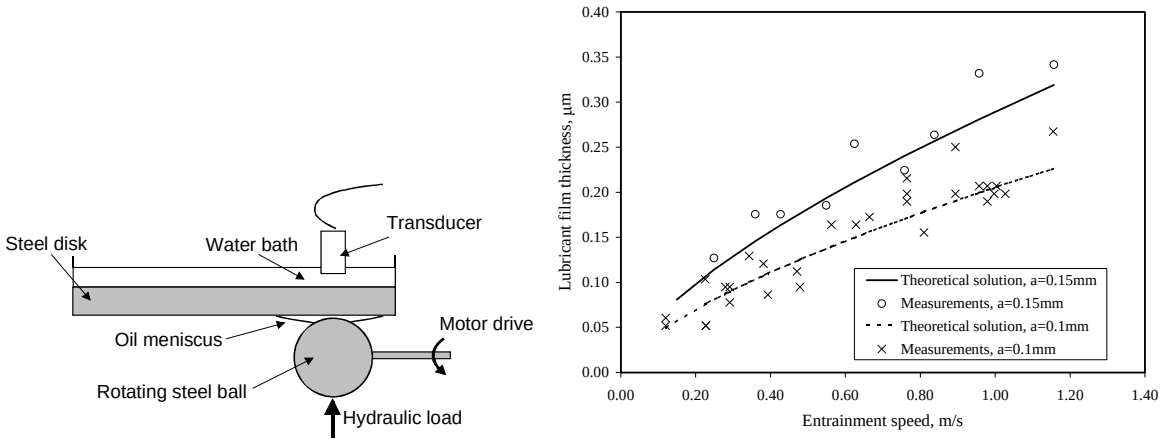

Figure 33. (a) Schematic diagram of apparatus used to generate an elastohydrodynamic film, and (b) measurement of film thickness for a sliding point contact (where *a* is the radius of the contact). Dwyer-Joyce et al. (2002).

A focusing system has also been used to measure the oil film thickness in a deep groove ball bearing (Dwyer-Joyce et al 2004a). The transducer was set to pulse continually and only reflected pulses that were reduced in amplitude (when the ball contact was directly incident) were stored and processed. Figure 34 shows the experimental apparatus and figure 35 shows a set of film measurements recorded for a variety of bearing loads and speeds.

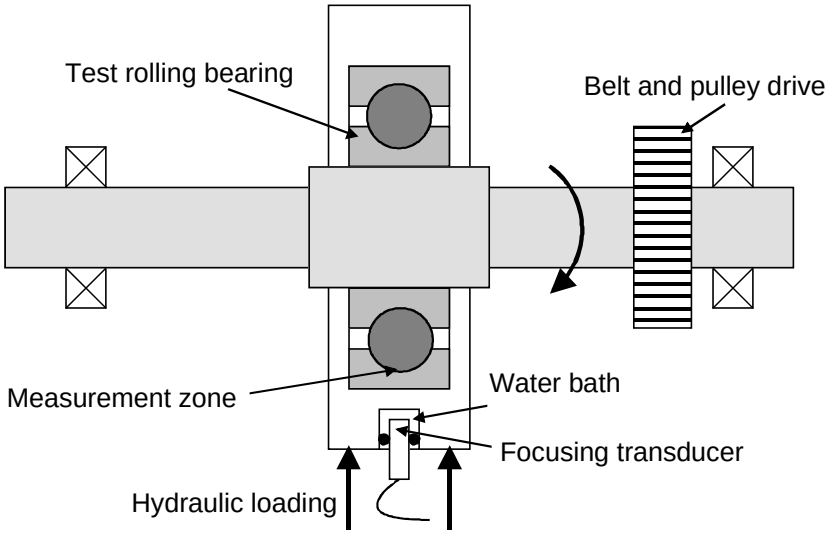

Figure 34. Schematic of apparatus used for ultrasonic measurements of film thickness in rolling element bearings. (Dwyer-Joyce et al 2004a).

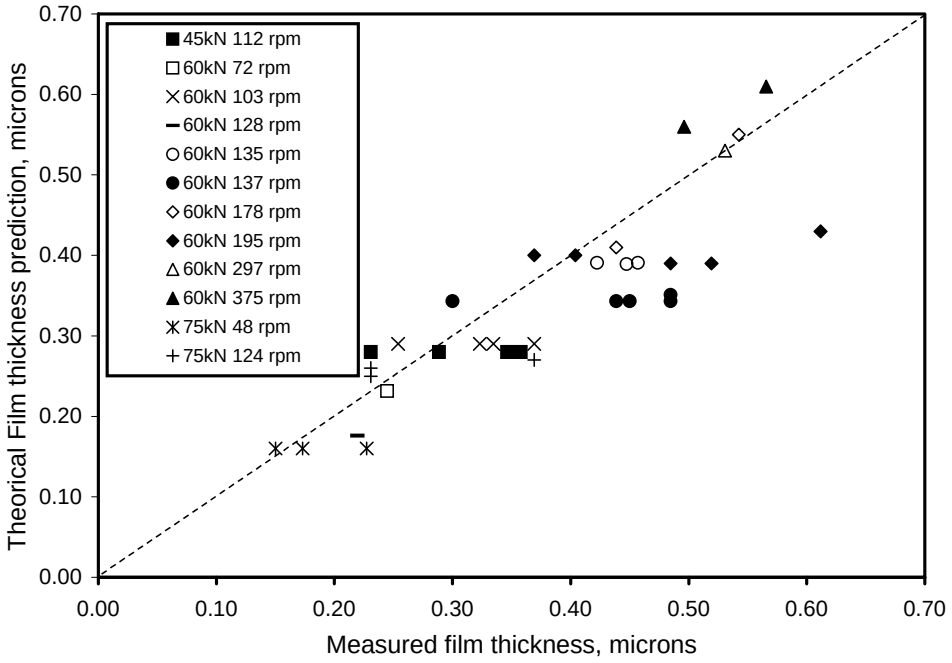

Figure 35. Comparison of rolling element bearing film thickness measured by an ultrasonic means with EHD theoretical solution (Dwyer-Joyce et al 2004).

The agreement between the measured film thickness and predictions based on elastohydrodyanmic theory is reasonable. It is not clear whether the variation in measured film (i.e. for a given load and speed) is caused by film variation in the bearing itself or repeatability of the technique. It should be noted that during these tests the temperature of the lubricant is not held constant (but rather rises as the bearing speed increases), thus one set of speed and load conditions can have two different values of predicted film thickness.

5. State of the Art and Prospects for the Future

The response of an interface to a low frequency ultrasonic wave is well understood. There are suitable mathematical models to describe the process and these models give a good interpretation of experimental results. However, measurements of the contact stiffness of dry contacts still differs somewhat from that predicted by both numerical and statistical models of contact. Whilst there is good qualitative agreement, ultrasonically measured stiffness is somewhat higher than predictions. It is not as yet possible to account for these discrepancies, and ultrasound has not been able to reveal with certainty how many asperities are actually in contact. Agreement between ultrasonic experimental measurements from lubricated contacts has been much easier to correlate with theoretical predictions.

There are second order effects at the interface (scattering, damping, and higher order reflections) that may also have an effect on ultrasonic response, especially at high frequencies. This is an area still under research and promises to be significantly more complex than the quasi-static approaches used to date. For most contacts found in engineering machine elements, it appears that this is not of concern and standard spring models give a satisfactory interpretation of results.

Both longitudinal and shear bulk waves have been used to investigate contacts. Essentially both have similar responses. However, the shear wave is fully reflected at a solid/liquid interface, whilst longitudinal waves are only partially reflected. The combination of normal and transverse waves promises to be a suitable technique for studying mixed liquid solid contacts found in boundary lubricated components.

The propagation of guided surface (Rayleigh) and plate (Lamb) waves has found many applications in the monitoring of solid structures. There has, as yet, been little work on this to study interfaces. This is another area with potential; as the actual contact area is frequently very small compared with the overall size of the machine element and locating it with a bulk ultrasonic wave is difficult. Perhaps ultrasonic excitation of a component surface could yield information about the interfaces.

The ultrasonic method has some significant advantages over electrical and optical based methods. Principally it has the potential to be used non-invasively without extensive modification to the components. However, there are some limitations. The spatial resolution is a primary issue. Many tribological contacts are small (millimetre scale) and it is necessary to focus the ultrasonic wave. The degree to which a wave can be focused depends on the frequency and the transducer design. But practically focusing down to less than 100μm spot size is difficult. This is clearly a limitation for smaller EHL type contacts. The transducer must be orientated and acoustically coupled such that the wave is normally incident and focused on the contact. Again, for smaller contacts this requires the use of careful positioning. Another important consideration is that of attenuation in the bearing materials. Polymers, elastomers, porous materials, and multi-phase materials may cause significant attenuation of the signal. In addition, inspection of equation (2) shows that, when the acoustic impedances of the two materials either side of the interface differ greatly, the reflection tends to unity. So the range of reflection coefficient over which changes in the interface properties can be studied is reduced. Ultrasonic measurements work best for contacting homogeneous metals. For attenuative materials or for contacting pairs of very different properties then the approach is more limited.

Not with standing these limitations, there are many industrial machine elements where ultrasonic measurements of the contact have proved useful. There has been considerable work on specimen based contacts, and recently several studies on actual components, albeit laboratory based. There is potential to use some of the techniques described here on industrial components in the field. The use of actively generated ultrasound in the field as a contact sensor is a challenge for the future. Condition monitoring has long relied on the detection of acoustic signals that follow a component failure. There is scope to extend the use ultrasound as a tool to continually monitor healthy contacts.

6. Conclusions

The response of an interface to an incident ultrasonic wave is well understood. Workers from the non-destructive testing community have developed several approaches to interpret reflected and transmitted signals. Their motivation has generally been the study of fatigue cracks or adhesive layers.

The quasi-static spring model is widely used to predict reflection or transmission. The interface stiffness is the dominating feature; and models describe the ultrasonic response well. The prediction of stiffness for a homogenous layer (e.g. a lubricant film) is straightforward. However, the stiffness of a rough surface contact is less easy to define; and is based on rough surface contact modelling and all the asperity scale problems that this introduces.

Nevertheless, there have been several valuable studies where ultrasound has qualitatively described mechanisms occurring in rough surface contact; including cyclic plasticity, adhesion, asperity contacts, and junction growth. A new method for the measurement of lubricant films is also a valuable contribution to tribology.

There are now several examples of ultrasonic based techniques being used in component tribology. This has provided new methods to measure contact pressure, real area of contact, sealing, and oil film thickness in machine elements. These applications have largely been laboratory based. However, they indicate a potential for field testing also, and the possibility of applications in machine element condition monitoring.

References

Ahn, H. and Kim, D., (2001), In-Situ Evaluation of Wear Surface by Ultrasound, Wear, Vol. 251, pp. 1193-1201.

Anderson, W., Jarzynski, J. and Salant, R.F., (2000), Condition Monitoring of Mechanical Seals: Detection of Film Collapse Using Reflected Ultrasonic Waves, Proceedings of the I.Mech.E., Part C Journal of Mechanical Engineering Science, Vol. 214, no. 9, pp. 1187-1194.

Anderson, W., Jarzynski, J. and Salant, R.F., (2001), A Condition Monitor for Liquid Lubricated Mechanical Seals, Tribology Transactions, Vol. 4, pp. 801-806.

Anderson, W., Salant, R.F. and Jarzynski, J., (1999), Ultrasonic Detection of Lubricating Film Collapse in Mechanical Seals, Tribology Transactions, Vol. 4, pp. 801-806.

Arakawa, T. (1983), A study on the transmission and reflection of an ultrasonic beam at machined surfaces pressed against each other, Materials Evaluation, 41, 714-719.

Baik, J-M., Thompson, R. B., (1985), Ultrasonic scattering from imperfect interfaces: a quasi-static model, Journal of Nondestructive Evaluation, 4, 177-196.

Baltazar, A., Rokhlin, S., and Pecorari, C., (2002), 'On the Relationship between Ultrasonic and Micromechanical Proerties of Contacting Rough Surfaces', Journal of the Mechanics and Physics of Solids, Vol. 50, pp. 1397-1416.

Birring, A.S. and Kwun, H., (1989), Ultrasonic Measurement of Wear, Tribology International, Vol. 22, pp. 33-37.

Biwa, S., Nakajima, S., Ohno, N., (2004), On the Acoustic Nonlinearity of Solid-Solid Contact With Pressure-Dependent Interface Stiffness, Transactions of the ASME, Journal of Applied Mechanics, in press.

Buck, O. Thompson, R. B., (1985), Ultrasonic scattering from imperfect interfaces: a quasi-static model, Journal of Nondestructive Evaluation, 4, 177-196.

Buck, O., Morris, W.L., and Richardson, J.M., (1978), Acoustic Harmonic Generation at Un-bonded Interfaces and Fatigue Cracks, Applied Physics Letters, Vol. 33, pp. 371-373.

Bush, A.W., Gibson, R.D., and Thomas, T.R., (1975), The Elastic Contact of a Rough Surface, Wear, Vol. 107, pp. 87-113.

Drinkwater, B. W., Castaings, M., and Hosten, B., (2003), The Measurement of A0 and S0 Lamb Wave Attenuation to Determine the Normal and Shear Stiffnesses of a Compressively Loaded Interface, Journal of the Acoustical Society of America, Vol. 113, pp. 3161-3170.

Drinkwater, B. W., Dwyer-Joyce, R. S. and Cawley, P., (1996), A study of the interaction between ultrasound and a partially contacting solid-solid interface, Proceedings of the Royal Society of London, Vol. 452A, pp. 2613-2628.

Drinkwater,B. and Cawley, P (1997), Measurement of the Frequency Dependence of the Reflection Coefficient from Thin Interface Layers and Partially Contacting Interfaces, Ultrasonics, Vol. 35, pp. 479-488.

Dwyer-Joyce, R. S., and Drinkwater, B. W., (1998), "Analysis of Contact Pressure Using Ultrasonic Reflection", Experimental Mechanics, Proceedings of the 11th International Conference on Experimental Mechanics, Balkema, Rotterdam, pp. 747-754.

Dwyer-Joyce, R. S., Drinkwater, B. W., and Quinn, A.M., (2001), "The Use of Ultrasound in the Investigation of Rough Surface Interfaces", ASME Journal of Tribology, Vol. 123, pp. 8-16.

Dwyer-Joyce, R.S., and Drinkwater, B., (2004a), 'Operating Limits for Acoustic Measurement of Rolling Bearing Oil Film Thickness', in press STLE Tribology Transactions.

Dwyer-Joyce, R.S., Drinkwater, B.W., and Donohoe, C.J., (2002), "The Measurement of Lubricant Film Thickness using Ultrasound", Proceedings of the Royal Society Series A, Vol. 459, pp 957-976.

Dwyer-Joyce, R.S., Harper, P., and Drinkwater, B., (2004b), 'A Method for the Measurement of Hydrodynamic Oil Films Using Ultrasonic Reflection', Tribology Letters, Vol. 17, pp. 337-348.

Greenwood, J. A. and Williamson, J. B. P., (1966), "Contact of Nominally Flat Surfaces", Proceedings of the Royal Society of London, Vol. 295A, pp. 300-319.

Haines, N. F., (1980), The theory of sound transmission and reflection at contacting surfaces, Report RD/B/N4744, Central Electricity Generating Board Research Division, Berkeley Nuclear Laboratories.

Hodgson, K., Dwyer-Joyce, R. S., and Drinkwater, B. W., (2000), "Ultrasound as an Experimental Tool for Investigating Engineering Contacts", Tribologia - Finnish Journal of Tribology, Vol. 19, No. 4, pp. 9-17.

Hosten, B., 1991, Bulk heterogeneous plane-wave propagation through viscoelastic plates and stratified media with large values of frequency-domain, Ultrasonics, Vol. 29, pp. 445-450.

Ito,Y., J. Toyoda and S. Nagata, (1979), Interface pressure distribution in a bolt-flange assembly, Transactions of the ASME, Journal of Mechanical Design, Vol. 101, 330-337.

Kendall, K. and Tabor, D., (1971), An ultrasonic study of the area of contact between stationary and sliding surfaces, Proc. R. Soc. Lond. Vol. 323A, pp. 321-340.

Kinra, V.K., Jaminet, P.T., Zhu, C. and Iyer, V.R., (1994), Simultaneous measurement of the acoustical properties of a thin-layered medium: The inverse problem, Journal of the Acoustical Society of America, Vol. 95, pp. 3059-3074

Kräutkramer, J. and Kräutkramer, H., (1975) Ultrasonic testing of materials, Springer-Verlag, New York.

Krolikowski, J. and Szczepek, J., (1992), Phase shift of the reflection coefficient of ultrasonic waves in the study of the contact interface, Wear, Vol. 157, pp. 51-64.

Krolikowski, J. and Szczepek, J., (1991), Prediction of contact parameters using ultrasonic method, Wear, Vol. 148, pp. 181-195.

Krolikowski, J. and Szczepek, J., (1993), Assessment of tangential and normal stiffness of contact between rough surfaces using ultrasonic method, Wear, Vol. 160, pp. 253-258.

Krolikowski, J., Szczepek, J. & Witczak, Z. (1989), Ultrasonic investigation of contact between solids under high hydrostatic pressure, Ultrasonics, Vol. 27, 45-49.

Lavrentyev, A. I. and Rokhlin, S. I., (1998), Ultrasonic spectroscopy of imperfect contact interfaces between a layer and two solids, Journal of the Acoustical Society of America, Vol. 103, pp. 657-664.

Lewis, R., Marshall, M.B., and Dwyer-Joyce, R.S., (2003), Ultrasonic Characterisation of an Interference Fit, Proceedings of the 29th Leeds-Lyon Symposium on Tribology, Elsevier, pp. 449-460.

Long, M. and Rack, H.J., (1997), Ultrasonic In-Situ Continuous Wear Measurements of Orthopaedic Titanium Alloys, Wear, Vol. 205, pp. 130-136.

Margetan, F.J., Thompson, R.B., Rose, J.H.M and Gray, T.A., (1992), The Interaction of Ultrasound with Imperfect Interfaces: Experimental Studies of Model Structures, Journal of Non-Destructive Evaluation, Vol. 11, pp. 109-125.

Marshall, M.B., Lewis, R., and Dwyer-Joyce, (2004a), Contact Pressure Measurement In Bolted Joints, Proceedings of the 12th International Conference on Experimental Mechanics, 2004 Politecnico di Bari, Italy

Marshall, M.B., Lewis, R., Drinkwater, B.W., and R.S. Dwyer-Joyce, R.S., (2004b), An Approach for Contact Stress

Mapping in Joints and Concentrated Contacts, Journal of Strain Analysis, Vol. 39, pp. 339-350.

Marshall, M.B., Lewis, R., Dwyer-Joyce, R.S., Olofsson, U. and Björklund, S., (2004c), Ultrasonic Characterisation of a Wheel/Rail Contact, Proceedings of the 30th Leeds-Lyon Symposium on Tribology, Elsevier. In press.

Masuko, M. and Ito, Y. (1969), Measurement of Contact Pressure by Means of Ultrasonic Waves, Annals of the CIRP, Vol 17, pp. 289-296.

Mott, G., and Taszarek, B.J., (1985), Ultrasonic Characterisation of an Interference Fit, Materials Evaluation, Vol. 43, pp. 990-994.

Nagy, P.B. and Adler, L., (1991), Reflection of Ultrasonic Waves at Imperfect Boundaries, Review of Progress in Quantitative Non-destructive Evaluation, Vol. 10, pp. 177-184.

Nagy, P.B., (1992), Ultrasonic classification of imperfect interfaces, Journal of Non-destructive Evaluation, Vol. 11, pp. 127-139.

Pau, M., Aymerich, F., and Ginesu, F., (2000), Ultrasonic Measurements of Nominal Contact Area and Contact Pressure in a Wheel-Rail System, Proceedings of the I.Mech.E., Part F Journal of Rail and Rapid Transit, Vol. 214, pp. 231-243.

Pau, M., Aymerich, F., and Ginesu, F., (2002), Distribution of Contact Pressure in Wheel-Rail Contact Area, Wear, Vol. 253, pp. 265-274.

Pau, M., (2003), Estimation of Real Contact Area in a Wheel-Rail System by Means of Ultrasonic Waves, Tribology International, Vol. 36, pp. 687-690.

Pialucha, T. and Cawley, P., (1994), The detection of thin embedded layers using normal incidence ultrasound, Ultrasonics, Vol. 32, pp. 431-440.

Polijaniuk, A. and Kaczmarek, J., (1993), Novel stage for ultrasonic measurement of real contact area between rough and flat parts under quasi-static load, ASTM Journal of Testing and Evaluation, Vol. 21, pp. 174-177.

Povey, M.J.W., (1997), Ultrasonic Techniques for Fluids Characterisation, Academic Press, San Diego.

Solodov, I.Y., (1998), Ultrasonics of Non-Linear Contacts: Propagation, Reflection, and NDE-Applications, Ultrasonics, Vol. 36, pp. 383-390.

Takeuchi, A., Sato, M. and Aoki, H., (1995), Local observation of solid friction by ultrasonic method, Proceedings of the International Tribology Conference, Yokohama, pp. 121-126.

Tattersall, A.G. (1973), The ultrasonic pulse-echo technique as applied to adhesion testing, J. Phys. D: Appl. Phys, Vol. 6, 819-832.

Thompson, R.B., Skillings, B.J., Zachary, L.W., Schmerr, L.W., and Buck, O., (1983), Effects of Crack Closure on Ultrasonic Transmission, Review of Progress in Quantitative Non-destructive Evaluation, Vol. 10, pp. 325-340.

Tsao, M.C., Grills, R.H., Simpson, R.P., and Andrew, G.A., (1984), Ultrasonic Colour Imaging and Stress Analysis of Piping Coupler Shrink Fits, Materials Evaluation, Vol. 42, pp. 1393-1400.

Webster, M. N. and Sayles, R. S., (1986), "A Numerical Model for the Elastic Frictionless Contact of Real Rough Surfaces", Transactions of the ASME, Journal of Tribology, Vol. 108, pp. 314-320.

Whitehouse, D. J. and Archard, J. F., (1970), "The Properties of Random Surfaces of Significance in their Contact", Proceedings of the Royal Society of London, Vol. 316A, pp. 97-121.

Wooldridge, A.B. and Steel, G., (1980), The Influence of Crack Growth Conditions and Compressive Stress on the Detection and Sizing of Fatigue Cracks, Report NW/SSD/RR/45/80, Central Electricity Generating Board, Manchester, England.

Wooldridge, A.B., (1979), The Effects of Compressive Stress on the Ultrasonic Response of Steel-Steel Interfaces and of Fatigue Cracks, Report NW/SSD/RR/42/79, Central Electricity Generating Board, Manchester, England.

Wooldridge, A.B., (1980), The Effects of Compressive Stress and Contaminating Liquids on the Ultrasonic Detection of Fatigue Cracks, Revue du CETHEDEC, Vol. 17, pp233-244.

Yoshioka, N. and Scholz, C.H., 1989, "Elastic properties of Contacting Surfaces Under Normal and Shear Loads 1: Theory", J. Geophys. Res., Vol. 94, pp. 17681-17690.

Yoshioka, N. and Scholz, C.H., 1989, "Elastic properties of Contacting Surfaces Under Normal and Shear Loads 2: Comparison of Theory with Experiment", J. Geophys. Res., Vol. 94, pp. 17691-17700.